Biochimica et Biophysica Acta 1783 (2008) 2398–2414

Contents lists available at ScienceDirect

Biochimica et Biophysica Acta

journal homepage: www.elsevier.com/locate/bbamcr

Chromatin structure influences the sensitivity of DNA to γ-radiation

Martin Falk, Emilie Lukášová *, Stanislav Kozubek

Institute of Biophysics, Academy of Sciences of the Czech Republic, Kralovopolska 135, 61265 Brno, Czech Republic

ARTICLE INFO

Article history:
Received 22 May 2008
Received in revised form 11 July 2008
Accepted 11 July 2008
Available online 25 July 2008

Keywords:
Chromatin structure
DNA damage
Double-strand break (DSB)
DNA repair
Experimentally changed radiosensitivity
Apoptosis

ABSTRACT

For the first time, DNA double-strand breaks (DSBs) were directly visualized in functionally and structurally different chromatin domains of human cells. The results show that genetically inactive condensed chromatin is much less susceptible to DSB induction by γ-rays than expressed, decondensed domains. Higher sensitivity of open chromatin for DNA damage was accompanied by more efficient DSB repair. These findings follow from comparing DSB induction and repair in two 11 Mbp-long chromatin regions, one with clusters of highly expressed genes and the other, gene-poor, containing mainly genes having only low transcriptional activity. The same conclusions result from experiments with whole chromosome territories, differing in gene density and consequently in chromatin condensation. It follows from our further results that this lower sensitivity of DNA to the damage by ionizing radiation in heterochromatin is not caused by the simple chromatin condensation but very probably by the presence of a higher amount of proteins compared to genetically active and decondensed chromatin. In addition, our results show that some agents potentially used for cell killing in cancer therapy (TSA, hypotonic and hypertonic) influence cell survival of irradiated cells via changes in chromatin structure and efficiency of DSB repair in different ways.

1. Introduction

Chromosomes are organized in territories which are non-randomly distributed in cell nuclei. In many human cell types, chromosome territories (CTs) have a radial organization [1–3]; however, the basic principles of chromatin folding in CTs are not yet clearly understood. A large body of evidence shows that the higher-order folding of chromatin fibres in CTs is closely related to genome function, in particular, transcription and replication [[4] and citations herein]. Recent experiments show that dynamic changes in chromatin structure in the vicinity of DSBs are required for their repair [5,6]. These changes reflect local chromatin decondensation connected with post-translational modifications of histones, and assembly of diverse proteins at the sites of chromosomal lesions [6,7].

Double-strand breaks (DSBs) in DNA occur frequently in the genome through the action of DNA-damaging agents or during genome replication [8]. They are hazardous for the cell because improper repair of them may lead to tumorigenic translocations [9]. The most dangerous translocations are those affecting proto-oncogenes, oncogenes, regulatory DNA sequences and genes. Since most coding genes occur in open chromatin [10,11], it is important to know whether this chromatin has greater sensitivity to DNA-damaging agents than condensed chromatin, which contains a low density of genes characterized by a low level of transcriptional activity. In other words, we wish to know how DNA damage is affected by chromatin structure and the architecture of the interphase nucleus. The influence of chromatin structure on the susceptibility of DNA to damage, and the efficiency of its repair in human lymphocytes, were indirectly deduced from the different yields of aberrations observed for individual chromosomes in mitosis [12,13]. There were more exchange aberrations in chromosomes that contained a higher density of genes. Although the results clearly show a higher risk of chromosomal translocations in gene-dense chromatin, they do not provide evidence of higher sensitivity of this open chromatin to the initial DNA damage, since not all DSBs give rise to exchange aberrations; indeed, most breaks are repaired correctly soon (several minutes) after their induction [14,15]. Therefore, the results described above, as well as other recent results, do not deal either with the induction or kinetics of DSB repair in different chromatin structures. Moreover, gene density and the expression of particular loci may differ according to the cell type studied, which requires further studies of the relationship between these factors.

The radial distribution of chromosomes in human interphase nuclei is correlated with gene density. The most gene-rich chromosomes are localized in the central part of the nucleus, whereas the gene-poor chromosomes occupy more peripheral positions close to the nuclear membrane [1,3]. This arrangement of chromosomes evidently has functional importance, because it correlates with gene expression [16]. Besides, it has been suggested that the radial organization could have a protective role for the genome [17]. Heterochromatic chromosomes located at the nuclear periphery might absorb mutagens as they enter the nucleus, and hence protect DNA in the central part of the nucleus from damage. This arrangement

* Corresponding author. Tel.: +420 541517165; fax: +420 541240498.
E-mail address: lukasova@ibp.cz (E. Lukášová).

0167-4889/$ – see front matter © 2008 Elsevier B.V. All rights reserved.
doi:10.1016/j.bbamcr.2008.07.010

would ensure the preferential protection of many coding sequences, since the most gene-rich chromosomes are located in the centre of the nucleus [17]. However, a protective effect of the radial arrangement of chromosomes against the oxidative effect of UV-C radiation was not found; indeed, more damage was induced in the nuclear centre than at the periphery [18]. On the basis of these findings, the authors suggested that the sequences located in the centre of the nucleus are more susceptible to damage. Again, these results do not show directly the influence of chromatin structure on sensitivity to DNA-damaging agents, but do show unequivocally that there are factors responsible for the non-homogeneous distribution of DSBs in the cell nucleus. Nowadays, the above mentioned questions can be addressed more directly and more precisely due to progress in microscopical and immunological techniques. The most convenient method for detection and nuclear localization of DSBs (the most dangerous DNA damage) immediately after their induction is the direct observation of phosphorylated H2AX (γH2AX), which accumulates specifically at sites of DSBs [19,20] and which can be visualized by specific antibody. By monitoring assemblage of repair proteins at DSB sites, this method allows the study of DSB repair during the period after damage induction, and quantification of the repair progress. In combination with fluorescence in situ hybridization (FISH), this method (Immuno-FISH, [21]) permits direct detection of DSBs and/or proteins participating in DSB repair, together with specific DNA sequences, and thus the time course of damage induction and repair can be studied.

To analyse the relationship between the susceptibility of DNA to DSBs and chromatin structure, we irradiated cells with γ-rays (used as a source of low linear energy transfer radiation), and followed DSB induction in two regions of the human genome that differed in their density of highly expressed genes. Clustering of the most highly transcribed genes into several domains called "RIDGEs" (regions of increased gene expression) was found in all tissues studied on the basis of expression profiles of chromosomal genes [10,11]. The genomic regions that are gene-poor and contain mainly genes that, if expressed, have only low transcriptional activity, were also identified and called "anti-RIDGEs". One RIDGE and one anti-RIDGE

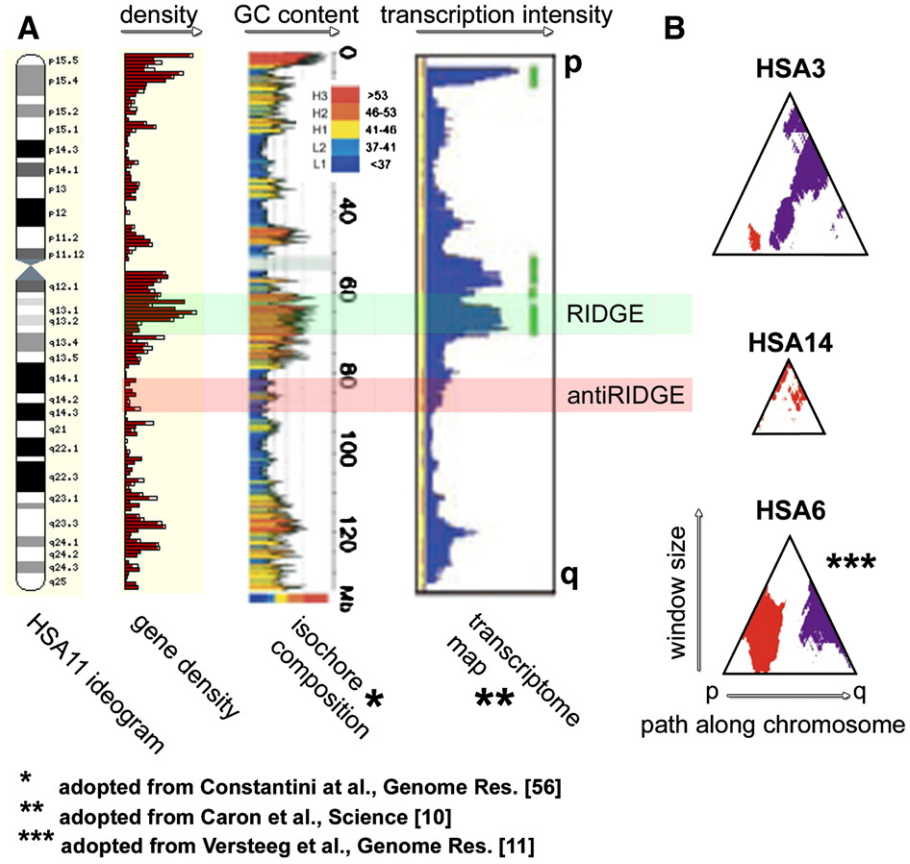

Fig. 1. The parameters used for characterization of chromosomes and specific chromosomal regions (RIDGE, anti-RIDGE) in this work. Efficiency of DSB repair and sensitivity to their induction were studied for chromosomes and specific chromosomal regions differing in their gene density (according to Ensembl database, released Mar 2008, http://www.ensembl.org/Homo_sapiens/mapview), isochore composition (according to Costantini et al., Genome Res. [56]) and gene transcription (adopted from Caron et al., Science [10] and Versteeg et al., Genome Res. [11]). Chromosome 11 containing both types of chromatin studied in this work – the clusters of highly expressed genes (RIDGEs, highlighted in green) and chromatin domains with very low expression (anti-RIDGEs, highlighted in red) – is used as an example (A). The overall gene density and transcription intensity follow from the graphs (in panel A). The vertical axis shows the path along the chromosome from p- to q-telomere (the position of genes/transcription units and isochore composition on the chromosome, respectively), the horizontal axis (from left to right) indicates increasing gene density, GC content and transcription intensity respectively. Most intensively expressed RIDGEs are labeled by the green bars (vertical), the RIDGE and anti-RIDGE clusters analysed in this work are highlighted in green and red respectively. The isochore composition of the whole chromosome and RIDGE and anti-RIDGE clusters follows from the middle graph: isochore L1 (ultramarine blue, GC-poorest), L2 (blue, GC=37–41%), H1 (yellow, GC=41–46%), H2 (orange, GC=46–53%), H3 (red, GC>53%). (B) "Ridgeograms" identifying chromosomal regions of significant extremes in gene expression and their clustering along DNA sequence (adopted from Rogier Versteeg et al., Genome Res. [11]). Transcription intensity was measured along the chromosome (horizontal axis, left: p-telomere, right: q-telomere) as the function of the window size (horizontal axis, starting with a window size 19 genes, at the base of the triangle, until the maximum possible window size for each chromosome at the top apex of the triangle). The ridgeograms show a tendency of highly (RED) and weakly (BLUE) expressed transcription units to form clusters along the DNA sequence, thus forming RIDGE (regions of increased gene expression) and anti-RIDGE clusters respectively (red and blue "spots" in ridgeograms respectively). Three types of RIDGE clusters can be distinguished on the ridgeograms: the RIDGEs consisting of a limited number of genes with very intensive expression (the upper triangle, e.g. HSA3), RIDGEs containing a large number of moderately expressed genes (the middle triangle, e.g. HSA14) and RIDGEs characterized by both very high expression level and a high number of genes (the bottom triangle, e.g. HSA6). For more details see [10, 11].

region of the same length (11 Mbp), both localized on 11q, were analysed in this work. DSB induction and repair in these regions were compared with those in selected nuclear territories of interphase chromosomes differing in their gene density (and content of RIDGEs) and consequently in chromatin condensation. To analyse whether simple changes in chromatin compaction alone (without participation of chromatin binding proteins) can influence DSB induction and repair efficiency, these processes were also studied after experimentally induced transient chromatin hyper- or hypocondensation by short (<10 min) incubation of cells in media with different osmolarities. The short exposure to high osmolarity leads to the immediate restoration of chromatin structure and cell functions and do not increase the annexin positivity of cells after their transfer to the normal (isotonic) medium. Hypertonic treatment of cells was described earlier as a method of reversibly modifying chromatin structure [22,23], sensitizing cells to chromosomal damage and killing by ionizing radiation [24]. Moreover, it was shown that injection of 7.2% saline into a carcinoma inhibited tumor growth [25]. High salt injections have also been used clinically for a wide variety of lesions including renal cysts, hemangioma and lumbar vertebral disks [25]. It is therefore of utmost importance to deeply analyse mechanisms by which higher osmolarity influences DNA sensitivity to DSB induction and repair. The influence of another promising enhancer of radiation therapy [26,27], histone deacetylase (HDAC) inhibitor trichostatin A (TSA), on DSB induction and repair was also investigated. While hyper/hypotonic treatment influences folding of the total nuclear chromatin, HDAC inhibitors, globally increase acetylation of histones, leading to reversible decondensation of dense chromatin regions [28].

2. Materials and methods

2.1. Cell culture, synchronization and irradiation

Human skin BJ fibroblasts, obtained from the American Type Culture Collection (Manassas, VA, USA), were grown in DMEM medium supplemented with 10% fetal calf serum (FCS), penicillin (100 I.E.) and streptomycin (100 μg/ml) at 37 °C with 5% CO_2. Synchronization of cells in the G_0 phase of the cell cycle was achieved by incubation of confluent culture without serum for 4 days. After trypsinization, cells were plated on microscope slides and incubated in the medium with 10% serum for 12 h before irradiation. During this period, more than 95% of cells were in the G_1 phase of the cell cycle [6]. Cells were irradiated with γ-rays from ^{60}Co with different doses: 1.0, 1.5, 3.0, 5.0 and 7 Gy (1 Gy/min). To explore the role of chromatin structure in radiosensitivity of cells, the osmolarity of the medium was changed 5 min before irradiation of cells, and maintained in this medium after irradiation 5–120 min before fixation. In another experiment, the irradiated cells, incubated for different periods of time in hyper- or hypoosmotic medium, were transferred to normal physiological medium, in which they were incubated for 10 min to 24 h before fixation.

2.2. Formation of medium with different osmolarities

The osmolarity of standard culture medium is 290 mOsm [23]. To obtain hypercondensed chromatin (HCC), the cells were incubated in a hyperosmotic medium (HOM) with an osmolarity of 570 mOsm. This medium was prepared by addition of 1 ml 20 × PBS (2.8 M NaCl, 54 mM KCl, 130 mM Na_2PO_4, 30 mM KH_2PO_4, pH 7.4) to 19 ml DMEM containing 10% FCS [23]. To reverse the effect, the cells were transferred directly to the standard physiological medium (290 mOsm); up to about 10–15 min the hyperosmotic (and also hypoosmotic) treatment has no effect on cell viability and all changes in chromatin structure and cellular processes were reversible. Hypocondensed chromatin in cells was obtained by cell incubation in hypoosmotic (HypoOM) medium. Hypoosmotic medium of about 140 mOsm was prepared by diluting standard culture medium with an equal quantity of sterile ddH_2O. Since chromatin condensation and decondensation started within seconds, washing in physiological salt solution before cell fixation was strictly avoided. The influence of HDAC inhibition on chromatin structure and cell radiosensitivity was studied by the addition of 1 μM or 0.2 μM trichostatin A (TSA) (Sigma-Aldrich, UK) to standard medium 12 h before irradiation, and keeping the cells in this medium for different periods of time after irradiation, prior to cell fixation.

2.3. Annexin positivity

An apoptosis detection kit (Sigma-Aldrich, UK) was used to detect the early stages of apoptosis in cells exposed to the hyperosmotic medium (570 mOsm). The principal component of this kit is annexin V-Cy3 that binds to phosphatidyl-serine (PS) if this is transposed to the external side of the plasma membrane. This transposition occurs at the onset of apoptosis, and thus makes the PS available for binding to annexin V. Binding was observed as red fluorescence. The procedure was performed on cells growing on microscope slides according to the manufacturer's recommendations. Living cells were stained green, due to their capacity to hydrolyse 6-carboxyfluorescein diacetate, which is the part of the kit.

2.4. Cell fixation and immunofluorescence staining of proteins

Cells were fixed with 4% formaldehyde in 1 × PBS for 10 min at room temperature (RT), washed several times in 1 × PBS, permeabilized with 0.2% Triton X 100/PBS for 15 min, and washed three times for 5 min in 1 × PBS. Before incubation with primary antibody (overnight at 4 °C), the cells were blocked with 7% inactivated FCS+2% bovine serum albumin/PBS for 30 min at RT. Antibodies from two different hosts (rabbit and mouse) were used to detect two different proteins in the same nuclei: anti-phospho-H2AX (serine 139), anti-phospho-ATM (1981), anti-HP1β, anti-acetyl-histone H4 lysine 5, and anti-dimethyl-histone H3 lysine 9 were from Upstate Biotechnology (Lake Placid, NY). Anti-phospho-NBS1 (serine 343) and anti-53BP were from Cell Signaling, anti-DNA-PK from Santa Cruz Biotechnology (CA, USA), and anti BRCA1, clone M4C7, from Millipore (MA, USA). Secondary antibodies were affinity purified FITC-conjugated donkey anti-mouse and Cy3-conjugated donkey anti-rabbit from Jackson Laboratory (West Grove, PA). The mixture of both antibodies was applied to each slide (after their pre-incubation with 5.5% donkey serum/PBS for 30 min at RT) and incubated for 1 h in the dark at RT. This was followed by washing (three times for 5 min each) in PBS. Cells were counterstained with 1 μM TOPRO-3 (Molecular Probes, Eugene, USA) in 2 × saline sodium citrate (SSC) prepared fresh from a stock solution. After brief washing in 2 × SSC, Vectashield medium (Vector Laboratories, Burlingame, CA, USA) was used for the final mounting of slides.

2.5. ImmunoFISH

ImmunoFISH was used to analyse the amount and localization of double-strand breaks (visualized as γ-H2AX foci) in the territories of human chromosomes HSA2, HSA4, HSA11, HSA18 and HSA19.

Fig. 2. Characteristics (A, B) of the five chromosomes (HSA2, HSA4, HSA11, HSA18 and HSA19) used for quantification of the chromatin density effect on the induction of DSBs by γ-radiation (dose of 3 Gy). (A) Gene density according to Ensemble database (orange) and isochore distributions for individual chromosomes from Costantini et al. [56] (GC content is expressed by different colors) (B) transcriptome maps (blue) and "ridgeograms" (triangles) are from Caron et al. [10] and Versteeg et al. [11] respectively (see Fig. 1 for more detailed explanation of these panels (A and B). (C) Images of fibroblast nuclei with simultaneously visualized (ImmunoFISH) territories of specific chromosomes (red; green for HSA11) and induced γH2AX foci (green; red for HSA11) detected 15 min PI.

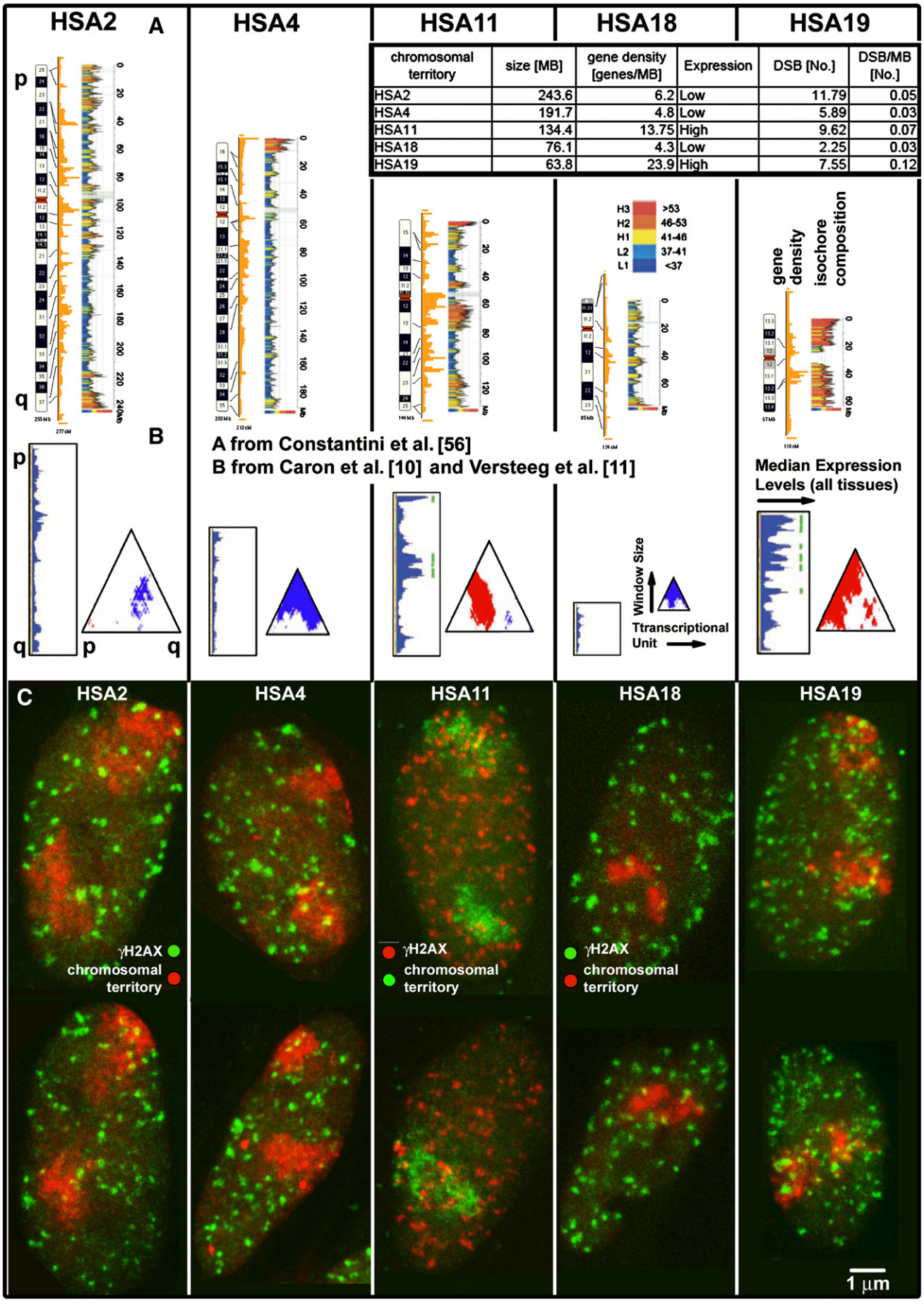

chromosomal territory	size [MB]	gene density [genes/MB]	Expression	DSB [No.]	DSB/MB [No.]
HSA2	243.6	6.2	Low	11.79	0.05
HSA4	191.7	4.8	Low	5.89	0.03
HSA11	134.4	13.75	High	9.62	0.07
HSA18	76.1	4.3	Low	2.25	0.03
HSA19	63.8	23.9	High	7.55	0.12

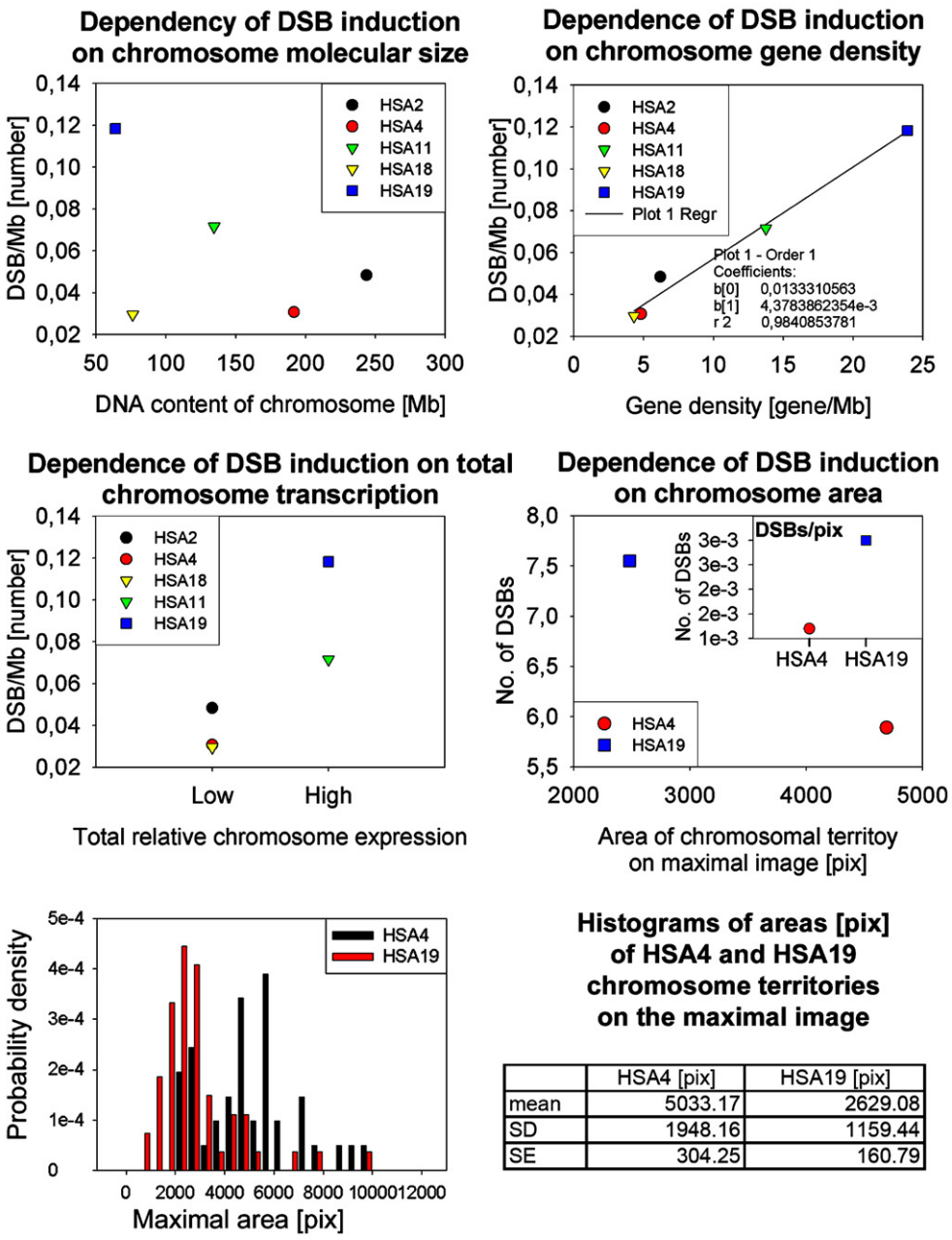

	HSA4 [pix]	HSA19 [pix]
mean	5033.17	2629.08
SD	1948.16	1159.44
SE	304.25	160.79

Fig. 3. Influence of different chromosomal parameters on the induction of DSBs by γ-radiation.

Chromosomes 19 and 18 (HSA19 and HSA18) were selected because of their contrasting characteristics and similar molecular size: HSA19 is genetically the most active chromosome in the human genome (human transcriptome map, [10]) with a decondensed, open chromatin structure; on the other hand, HSA18 is characterized by a very low transcription level and very compact chromatin. HSA2 is a chromosome with intermediate parameters, whereas HSA11 and HSA4 are further examples of active/decondensed and inactive/condensed chromosomes respectively. The level of DSB damage was also studied in two genomic regions with a known density of highly expressed genes and with well defined chromatin structure [4]. The RIDGE region (R) contains a large number of highly expressed genes and markedly decondensed chromatin, in contrast to the gene-poor and condensed anti-RIDGE (AR) region. Chromatin in this region is about 40% more condensed than in a RIDGE ([4] and our unpublished results). The size of both regions is 11 Mbp, both are located at 11q and separated by 12 Mbp.

Fig. 4. Comparison of chromatin texture in the territories of HSA19, containing a high density of highly expressed genes, and HSA4, with a low density of genes having generally low expression. (A) Upper: nuclei show the location of HSA4 and HSA19 territories (red) in nuclei of human fibroblasts irradiated with a dose of 3 Gy and subjected to immunoFISH 15 min PI. γH2AX foci are green. Lower: series of enlarged images of the HSA4 and HSA19 territories showing nuclear chromatin condensation as the intensity of TOPRO-3 (blue); or grey; merged images of chromosomal territories (CTs) and nuclear chromatin (red); and chromosomal territories alone (red). Different intensities of red show chromatin compaction in the chromosome territory. Green foci indicate the location of DSBs. It can be seen that these foci are predominantly located in regions of low chromatin density (faintly labeled by TOPRO-3, or red color of CTs). (B) Comparison of γH2AX foci location after immunodetection without denaturation of chromatin (Immuno) and after immunoFISH including chromatin denaturation (ImmunoFISH). Merging the two upper images shows that the location of γH2AX foci is almost unchanged after immunoFISH. (C) Optical slices through the territory of HSA4 (red) in *z*-steps of 0.2 μm, showing the location of γH2AX foci (green) in the region of low chromatin density (faintly red).

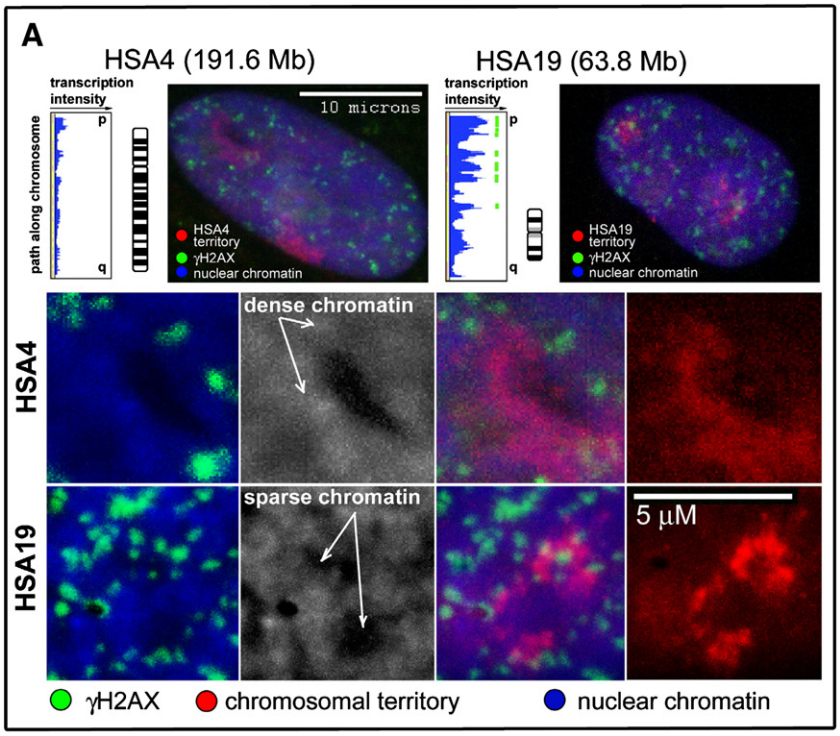
A
HSA4 (191.6 Mb)
HSA19 (63.8 Mb)
transcription intensity
path along chromosome
p
q
10 microns
HSA4 territory
γH2AX
nuclear chromatin
HSA19 territory
dense chromatin
sparse chromatin
5 μM
HSA4
HSA19
γH2AX
chromosomal territory
nuclear chromatin

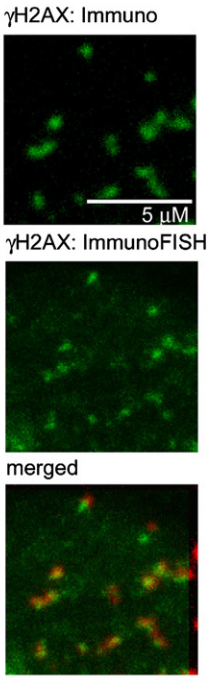
B
γH2AX: Immuno
5 μM
γH2AX: ImmunoFISH
merged

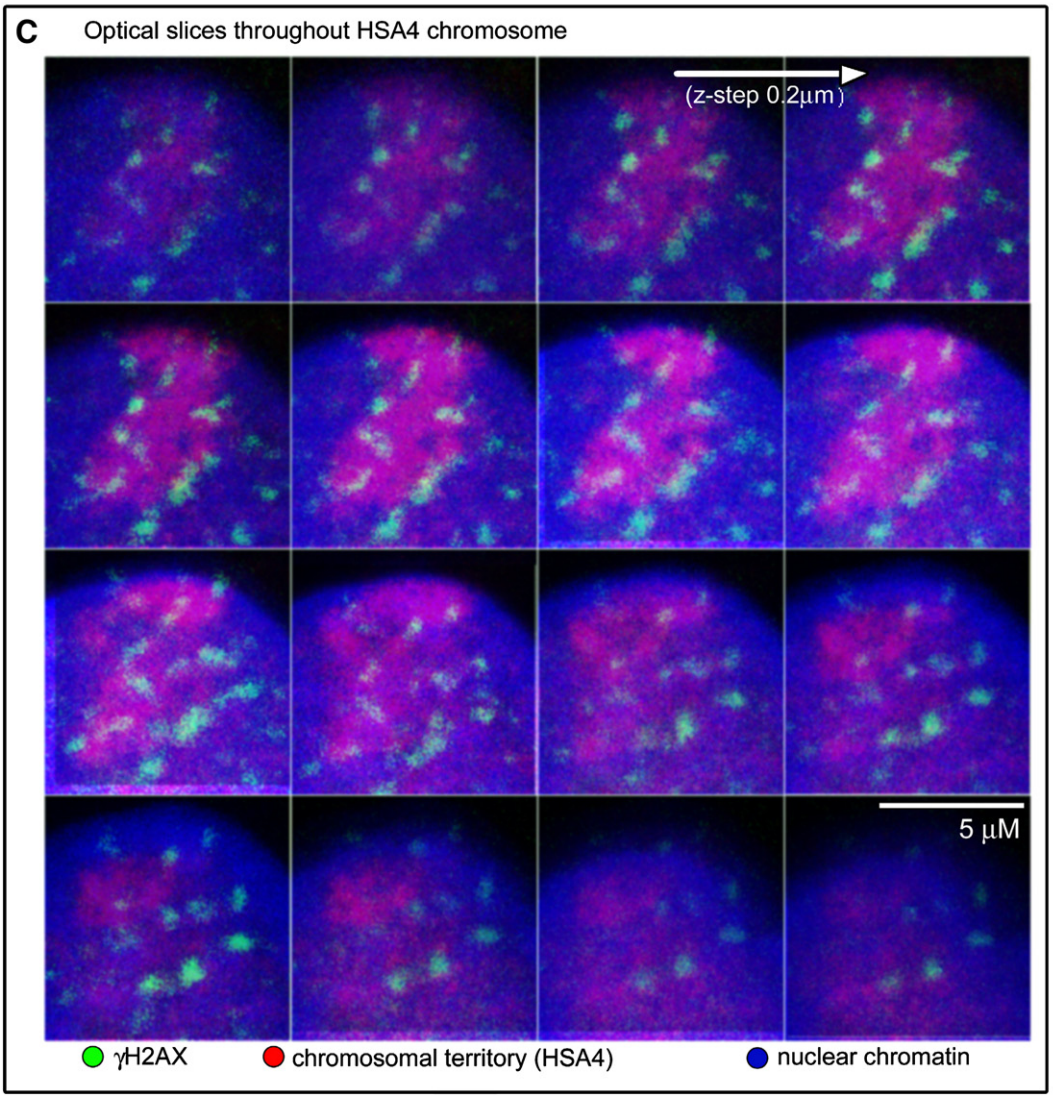
C
Optical slices throughout HSA4 chromosome
(z-step 0.2μm)
5 μM
γH2AX
chromosomal territory (HSA4)
nuclear chromatin

Directly labeled painting probes (Appligene-Oncor, Illkirch, France) for visualization of whole chromosomal territories were treated before hybridization according to the manufacturer's instructions. The probes for RIDGE and anti-RIDGE regions, conjugated with digoxigenin and biotin respectively, were obtained from S. Goetze (Swammerdam Institute of Live Sciences, University of Amsterdam). The immunoFISH protocol was adopted from [21] with slight modifications. In brief, the cells, on slides, were fixed in 4% formaldehyde/0.1% Triton X 100 for 30 min at 4 °C, followed by inactivation of aldehyde groups in 100 mM glycine/PBS for 20 min. Cells were permeabilized in 0.5% Triton X 100/0.5% saponin in PBS for 1 h and washed (3×5 min) in PBS. Before incubation overnight at 4 °C with antibody for γH2AX, the cells were blocked with 5% FCS/PBS for 30 min. Washing (3×5 min) in PBS preceded blocking with 5% donkey serum/PBS for 30 min and incubation with secondary antibody for 1 h, followed by washing in PBS (3×5 min). To fix the antibody before cell denaturation, the slides were immersed in 4% formaldehyde/0.1% Triton X 100 for 30 min at 4 °C, followed by inactivation of aldehyde groups in 100 mM glycine/PBS for 20 min. Cells were permeabilized in 0.5% Triton X 100/0.5% saponin in PBS for 35 min, washed in PBS (3×5 min), treated with 0.1 M HCl for 18 min, washed (3×5 min), and incubated in 20% glycerol for 15 min, and then in 2 × SSC for 10 min. Denaturation was performed in 70% formamide/2 × SSC (pH 7) for 3 min, followed by 50% formamide/2 × SSC for 1 min, both at 74 °C. The probes were denatured separately at 75 °C for 10 min, preannealed for 30 min at 37 °C and applied to denatured cells on slides. After hybridization overnight, slides were washed, and chromatin was stained with TOPRO-3 and mounted in Vectashield (Vector Laboratories, Burlingame, CA, USA). The slides labeled with RIDGE or anti-RIDGE probes conjugated with digoxigenin or biotin were blocked with 7% FCS/2% BSA for 30 min before detection with anti-digoxigenin-Cy3 and streptavidin-FITC, respectively, for 1 h at RT, followed by washing in 4 × SSC/0.1% Tween 20 at 37 °C (3×5 min), chromatin labeling, and mounting in Vectashield.

2.6. Image acquisition and confocal microscopy

An automated Leica DM RXA fluorescence microscope, equipped with a CSU10a Nipkow disc (Yokogawa, Japan) for confocal imaging, a CoolSnap HQ CCD-camera (Photometrix, Tucson, AZ, USA) and an Ar/Kr-laser (Innova 70C, Coherent, Palo Alto, CA) and an oil immersion Plan Fluotar objective (100×/NA1.3) was used for image acquisition [29,30]. Automated exposure, image quality control and other procedures were performed using FISH 2.0 software [29,30]. The exposure time and dynamic range of the camera in the red, green and blue channels were adjusted to the same values for all slides to obtain quantitatively comparable images. Forty serial optical sections were captured at 0.2 μm intervals along the z-axis at a constant temperature of 26 °C.

3. Results

3.1. DSB induction in chromatin containing different amounts of highly expressed genes

3.1.1. The dependence of DSB induction on chromosome gene density

The sensitivity of DNA to DSB induction was compared for five chromosomes, differing in their molecular size (DNA content, [Mbp]), isochore composition, gene density, the number of highly transcribed genes, the overall level of transcription and consequently their chromatin structure; these parameters are explained in Fig. 1 and the characteristics of all the chromosomes studied are summarized in Fig. 2A, B. DSB induction and the consequent repair process were studied by means of immunoFISH, enabling direct visualization of γH2AX foci, the markers of DSB, together with individual interphase chromosomal territories (Fig. 2C).

In correlation with the highest gene density (23.9 genes/Mbp), overall expression activity and number of intensely expressed genes of HSA19 (Fig. 2A, B), irradiation of cells with γ-rays induced the largest number of DSBs per megabase pair of all the chromosomes analysed within the territory of this chromosome (0.12 DSB/Mbp) (Figs. 2C and 3). The gene density of HSA11 is still high, but nevertheless about half that of HSA19 (13.75 genes/Mbp); on the other hand, its molecular size, 134.4 Mbp, is about twice that of HSA19 (63.8 Mbp) (table in Fig. 2A). Interestingly, the mean number of DSBs induced under the same conditions inside the territory of HSA11 was about half (0.07 DSB/Mbp) that of HSA19 (Figs. 2C and 3).

HSA18 has a very low density of genes (4.3 genes/Mbp, Fig. 2A) and does not contain highly expressed genes at all (Fig. 2B). Despite being about the same molecular size as HSA19 (76.1 Mbp), the mean number of DSBs induced inside the territory of this chromosome was a quarter of that for HSA19 (0.03 DSB/Mbp) (Fig. 3). The molecular size of HSA4 is about three times larger (191.7 Mbp) than that of HSA18, but its gene density is almost the same (4.8 genes/Mbp) (Fig. 2A). Reflecting the latter parameter, the mean number of DSBs induced inside the territory of HSA4, normalized to one megabase of DNA, was the same (0.03 DSB/Mbp) as in HSA18 (Fig. 3).

The largest chromosome analysed in this study was HSA2 (243.6 Mbp). Its gene density is rather low (6.2 genes/Mbp), but still about a third higher than that of HSA4 and HSA18 (Fig. 2A, B). In accordance with the gene density of chromosomes analysed, the mean number of DSBs induced in the territory of HSA2 was higher (0.05 DSB/Mbp) than that in HSA18 and HSA4, but significantly lower than that in HSA11 and HSA19 (Fig. 3).

Taken together, these results show unequivocally that the mean number of DSBs induced inside the chromosome territory correlates predominantly with the gene density of the chromosome, but not with the molecular size (DNA content) or nuclear size (the volume of chromosome territory in an interphase nucleus) (Fig. 3).

3.1.2. DSB induction in RIDGE and anti-RIDGE regions of HSA11

When total nuclear chromatin was counterstained with TOPRO-3, DSBs immunodetected as γH2AX foci appeared more frequently (about 70%) in faintly labeled nuclear areas, representing decondensed chromatin domains or nuclear space with a low chromatin concentration (Fig. 4).

To confirm the results for five different chromosomes described above, we studied the level of DSB damage in two genomic regions, a RIDGE and an anti-RIDGE, with known densities of highly expressed genes and with well defined chromatin structure (Fig. 5A, our unpublished results). In these experiments, the cells were irradiated with higher doses (7 Gy) of γ-rays to produce a number of DSBs sufficient for statistical comparison in each 11 Mbp region analysed. Even after this higher dose, a large fraction of surviving and normally repairing cells remained, as verified by annexin labeling (not shown) and monitoring of DSB repair during the post-irradiation (PI) period (Fig. 5B, left panel). The mean number of DSBs induced, counted 15 min PI was 7.93±0.32 in the RIDGE and a quarter of this (1.90±0.02 DSBs) in the anti-RIDGE (Fig. 5B). This result clearly shows that γ-radiation preferentially damages DNA in regions of open, decondensed chromatin.

3.2. Influence of chromatin structure on DSB repair

The influence of chromatin structure on the efficiency of DSB repair was studied by monitoring the decrease in DSB number 4 h PI. During this period, 80.6% of DSBs induced in the RIDGE, but only 52% of those in the anti-RIDGE, were repaired (Fig. 5B, left panel), indicating that the efficiency of DSB repair is also dependent on chromatin structure. A higher rate of DSB repair was also observed in gene-dense chromosomes (HSA19, HSA11) than in those with a low number of genes (HSA18, HSA4) (Fig. 6A, B). Similar to the

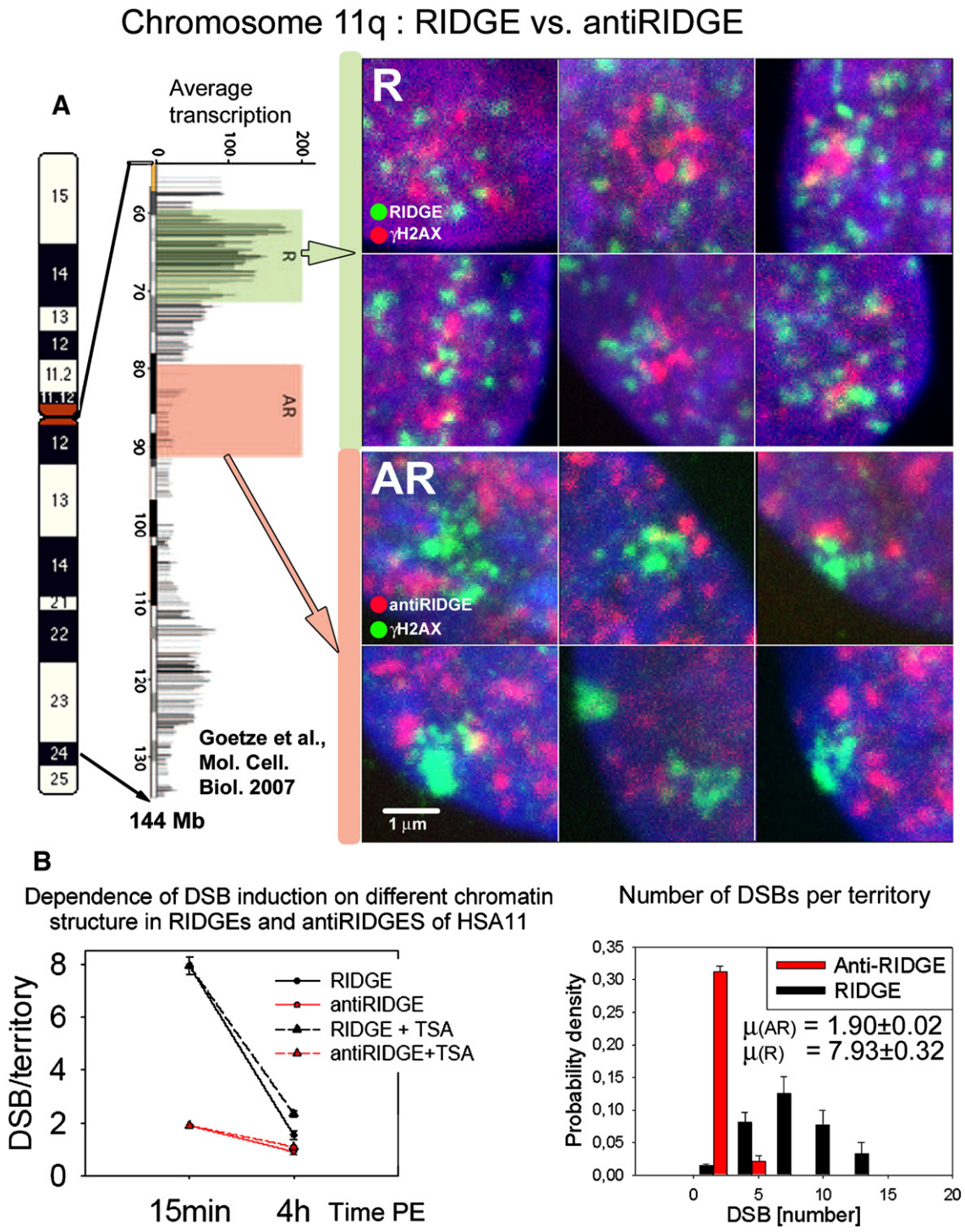

Fig. 5. DSBs induction and efficiency of repair in RIDGE and anti-RIDGE (both located in 11q) in human fibroblasts irradiated with a dose of 7 Gy of γ-rays. (A) Left: chromosome 11 ideogram and human transcriptome map of HSA11 (from Goetze et al. [4]) showing localization and transcriptional activity of the RIDGE and anti-RIDGE regions studied. Right: images R display the location and number of γH2AX foci (green) in RIDGE territories (red) of six nuclei, visualized together by immunoFISH. Images AR display the same for γH2AX foci (red) in relation to anti-RIDGE regions (green). (B) Graph: differences in DSB induction and repair during 4 h PI between the RIDGE and anti-RIDGE regions in cells incubated in ISO medium (full lines) and in the presence of 1 μm TSA 12 h before irradiation (dashed line). The histogram shows the distribution of DSBs per territory of RIDGE and anti-RIDGE, 15 min PI; μ indicates the mean values ± standard error.

values measured for the RIDGE, about 78% of DSBs were already repaired in HSA19 at 4 h after irradiation of the cells with 3 Gy (Fig. 6B). In other chromosomes, these values were 77% in HSA11, 69% in HSA2, 65% in HSA4, and 60% in HSA18 (Fig. 6B, C). It is obvious, therefore, that the rapidity of DSB repair in different chromosomes is correlated with their gene density, and consequently their chromatin structure.

3.2.1. Effect of HDAC inhibition with TSA on the induction and repair of DSBs in chromatin of different gene density

Incubation of cells with 1 μM trichostatin (TSA) before (12 h) and during γ-irradiation did not affect the mean number of DSBs induced, either in chromosomes with a high density of genes (HSA19, HSA11) or in the RIDGE (Figs. 6A and 5B respectively); the

same number of DSBs was also induced in the anti-RIDGE in treated and control cells (Fig. 5B) On the other hand, TSA treatment surprisingly increased the mean number of DSBs induced in chromosome territories containing a low density of genes (Fig. 6A). The efficiency of DSB repair was nevertheless slowed down by TSA in all chromosomes, as well as in the RIDGE and anti-RIDGE

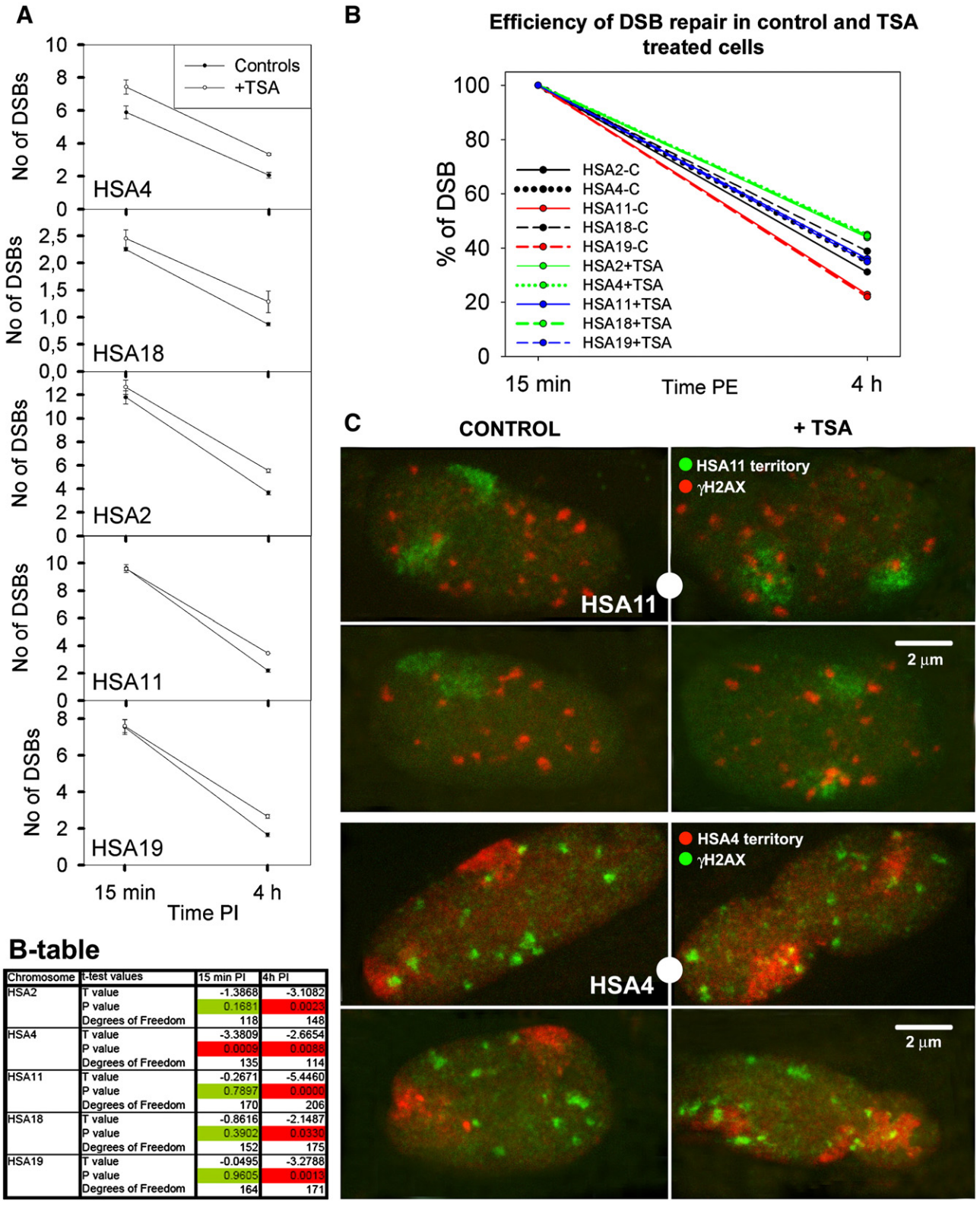

B-table

Chromosome	t-test values	15 min PI	4h PI
HSA2	T value	-1.3868	-3.1082
	P value	0.1681	0.0023
	Degrees of Freedom	118	148
HSA4	T value	-3.3809	-2.6654
	P value	0.0009	0.0088
	Degrees of Freedom	135	114
HSA11	T value	-0.2671	-5.4460
	P value	0.7897	0.0000
	Degrees of Freedom	170	206
HSA18	T value	-0.8616	-2.1487
	P value	0.3902	0.0330
	Degrees of Freedom	152	175
HSA19	T value	-0.0495	-3.2788
	P value	0.9605	0.0013
	Degrees of Freedom	164	171

Fig. 6. Influence of 1 μm TSA on DSB induction and repair in five chromosomes with different gene densities. (A) Induction and decrease of the mean number of DSB per chromosome territory during 4 h of cell incubation in isotonic medium post-irradiation, and in the medium supplemented with 1 μm TSA for 12 h before irradiation and 4 h PI. (B) Efficiency of DSB repair in five chromosomes with different gene density during cell incubation in isotonic medium for 4 h PI, and in cells treated with 1 μm TSA for 12 h before irradiation and 4 h PI. Table: statistical significance of the differences in DSB induction (15 min PI) and repair (4 h PI) between the cells growing in normal medium and that exposed to 1 μm TSA; green: $P > 10^{-2}$, red: $P < 10^{-2}$. (C) Images of HSA11 (green) and HSA4 (red) territories with the localization of γH2AX (red or green, respectively) in these territories.

regions (Figs. 6A, B, C and 5B respectively). Moreover, the efficiency of repair decreased more markedly in the RIDGE region (from 80.6% to 70.5%) than in the anti-RIDGE (from 52% to 45%) (Fig. 5B) and similar, but not so striking, results were also obtained for chromosomes with high and low concentrations of expressed genes (Fig. 6). The efficiency of repair decreased from 77.83% to 67.83% in HSA19, from 77.8% to 64% in HSA11, from 69% to 54% in HSA2, and from about 65% to 56% in HSA4 and HSA18, respectively. It seems therefore, that the sensitizing effect of TSA on DSB induction predominates in condensed, genetically silenced regions of the human genome, whereas its effect on inhibition of DSB repair takes place throughout the nucleus, but mainly in highly expressed chromatin domains.

3.3. DSB induction and repair in nuclei with experimentally changed chromatin condensation

3.3.1. Chromatin condensation

Hyperosmotic treatment is known to condense chromatin, inhibit tumor growth and sensitize cells to radiation. To determine whether these effects are functionally related, we have studied the influence of hyperosmotic-forced chromatin compaction on induction of DSBs by ionizing radiation and their repair post-irradiation (PI). We have addressed also another important question, whether the simple chromatin condensation provoked by hyperosmotic conditions without participation of additional proteins corresponds with our results obtained for functionally and structurally different chromatin domains in situ under physiological conditions. We studied the formation of γH2AX foci in human fibroblasts with experimentally changed chromatin condensation, using an approach first described by [31,32]. It allows the transient induction of hypercondensed chromatin (HCC) in living cells by increasing the osmolarity of the culture medium (290 mOsm). Our results show that, contrary to prolonged treatments, the short-time incubation (about 10 min) of cells in HOM does not influence the cell viability (Fig. 7A, B).

The hyperosmotic (HOM) treatment of cells for 10 min (HOM-cells$_{10\ min}$) resulted in marked changes in chromatin texture in the whole nucleus, manifested as branched bundles of hypercondensed chromatin (HCC) surrounded by extensive interchromatin space (as seen in Fig. 7C, middle nucleus). If HOM-cells were γ-irradiated with 1.0 or 3.0 Gy in HOM and left to repair their DNA under these conditions for 10 min, only small dots of γH2AX and repair proteins such 53BP (Fig. 7C, middle nucleus), NBS1, MDC1, ATM, BRCA1 etc. (not shown) were seen, dispersed through the nucleus, instead of the larger foci observed in normal isotonic (ISO) medium (Fig. 7, the first nucleus). The transfer of irradiated HOM-cells$_{10\ min}$ into isotonic medium for the next 10 min (HOM-ISO-cells$_{10+10\ min}$) led to complete restoration of chromatin structure, as well as the formation of γH2AX foci, showing phosphorylation of H2AX histones and assembly of repair proteins at these sites of damage (see Fig. 7C, right nucleus, for 53BP, not shown for NBS1, ATM, BRCA1 etc.), and thus reversibility of the structural and physiological changes induced by HOM (Fig. 7C, compare the left and right nucleus). Surprisingly, the sensitivity of hypercondensed chromatin to DSB induction by γ-radiation did not differ from chromatin in normal cells (P=0.68, Fig. 7D, compare also the left and right nucleus at Fig. 7C). Cells incubated for 10 min in HOM, irradiated during this time with 1.5 Gy and left to repair for the next 10 min in normal medium, had about the same number of DSBs (26.20±2.30) as in controls (26.35±1.35, Fig. 7D); equivalent results were obtained for irradiation of cells with 3 Gy (7D, histogram). Also, quantification of the disappearance of γH2AX foci in HOM-cells$_{10\ min}$ at different periods of time after their transfer to normal medium (Fig. 7E) revealed a very similar rate of DSB repair to control cells.

On the other hand, prolonged incubation of irradiated cells in HOM (15–60 min) was reflected in the formation of new γH2AX foci, the size and number of which progressively increased with time of incubation (Figs. 7A and 8A, B). γH2AX foci were formed even in non-irradiated cells during a prolonged incubation in HOM, indicating induction of DSB under these conditions (Fig. 9A) However, the formation of γH2AX foci was not followed by assembly of repair complexes and colocalization of foci with repair proteins in HOM (Figs. 8A and 9A for 53BP, not shown for NBS1, BRCA1, ATM etc.). In addition, the number of cells positively labeled for annexin increased concomitantly with the time of incubation in HOM, indicating a growing fraction of cells at the beginning of apoptosis (as already shown at Fig. 7A). The loss of vitality of cells exposed to HOM for long time is manifested also by their inability to restore the chromatin structure when transferred to normal medium (Fig. 9A).

These results show that short incubation (<10 min) of cells in HOM during and after irradiation induces reversible changes of chromatin structure and stalling of DSB repair; however, cells treated in this medium for longer were unable to repair DSB damage, and were forced into apoptosis even when transferred to isotonic medium.

3.3.2. Chromatin decondensation

The influence of chromatin decondensation on DSB induction and repair was studied in hypoosmotic medium (HypoOM, 140 mOsm). Surprisingly, HypoOM-treated cells for 10 min developed a chromatin texture similar to that induced by HOM: bundles of intensely labeled condensed chromatin distributed through the nucleus. However, these bundles were wider (swollen), and the nuclear space encompassing these bundles was largely filled with chromatin of low density (Fig. 8C), in contrast to the wide interchromatin space formed in HOM. Moreover, unlike to the rapid restoration of chromatin structure in cells incubated for 10 min in HOM, the similar chromatin texture that developed in cells treated with HypoOM only slowly returned to the normal state after their transfer into normal medium (Fig. 8C).

The mean number of DSBs induced per cell irradiated with a dose of 1.5 or 3 Gy and incubated in HypoOM for 10 min (irradiation during the fifth minute of incubation) was significantly higher (31 and 45.4 respectively, P=3.50e^{-5} for 1.5 Gy) than that induced in cells incubated in normal isotonic medium (26.5 and 38.7 respectively) (Fig. 7D). Moreover, DSB repair in HypoOM-cells$_{10\ min}$ was evidently slower than in control cells (Fig. 7E). While the mean number of DSBs per nucleus fell to 7.86 in controls (irradiated with 1.5 Gy) at 4 h PI, in cells incubated for 10 min in HypoOM prior to their transfer to normal medium for 4 h this value only dropped to 10.41 DSBs/nucleus. Compared with cells not exposed to HypoOM, 10 min incubation in this medium before replacing cells in normal medium resulted in a higher fraction of cells containing breaks (usually 1 or 2) even at 24 h PI (Fig. 8D). These results indicate higher sensitivity of chromatin decondensed by HypoOM to DSB induction, and a reduction of DSB repair long after the initial short incubation in HypoOM. However, despite these observations, and contrary to HOM-cells$_{10\ min}$, the majority of γH2AX foci colocalized with repair proteins even in HypoOM medium (Fig. 8C).

3.3.3. DSB induction and repair in the presence of trichostatin A

If human fibroblasts were cultured for 12 h before and 10 min after irradiation (1.50 or 3.0 Gy) in normal medium containing 0.2 μM or 1 μM TSA, the mean number of DSBs counted was slightly higher than in control cells (29.6±1.1 and 29.0±1.0 respectively, Fig. 7D). Surprisingly, while this number of DSBs differed significantly from that in normal medium only in the case of 1 μM TSA (P=0.19 and 0.05 for 0.2 μM and 1.0 μM TSA, respectively, in contrast to P=3.50e^{-5} after the HypoOM treatment), the repair of DSB damage was reduced considerably at both drug concentrations (Fig. 7E). Even 24 h after the cell irradiation (1.5 Gy), a large fraction of cells remained (88.5%, s.d.=4.4%) that contained two or more unrepaired DSBs in TSA-treated (1 μM) cells, whereas only 34.8% (s.d.=8.7%) of nuclei were DSB-positive (containing 1 to 2 breaks) in controls (Fig. 8D). Moreover, if repair proceeded in the absence of TSA following incubation with this drug (1 μM) for 12 h before and 10 min after irradiation, the fraction of DSB-positive cells was reduced to 58.8%

(s.d.=8.0%) (Fig. 8D), which is still significantly above the control level and is about the same as in cells irradiated and incubated in HypoOM for 10 min PI before their transfer to normal medium. Colocalization of γH2AX foci with repair proteins was not disrupted in TSA-treated cells and started early after irradiation, similarly to the HypoOM-treated cells and contrary to the HOM-treated cells. Together, these results show that short incubation of cells in TSA hinders the repair of DSBs, similarly to HypoOM, but does not markedly influence the number of radiation-induced DSB lesions (Fig. 7D, E). Moreover, contrary to HypoOM, TSA treatment induced less distinct changes in chromatin structure. Chromatin texture visualized by TOPRO-3 staining (Fig. 8C) consisted of a more

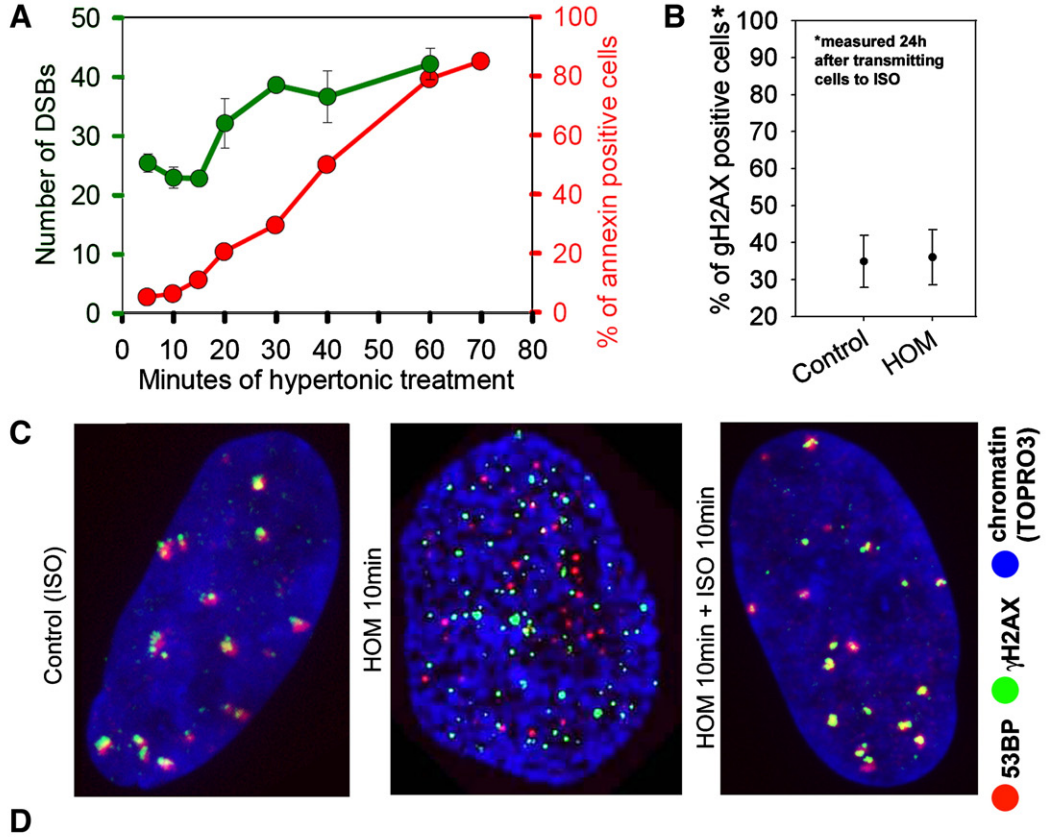

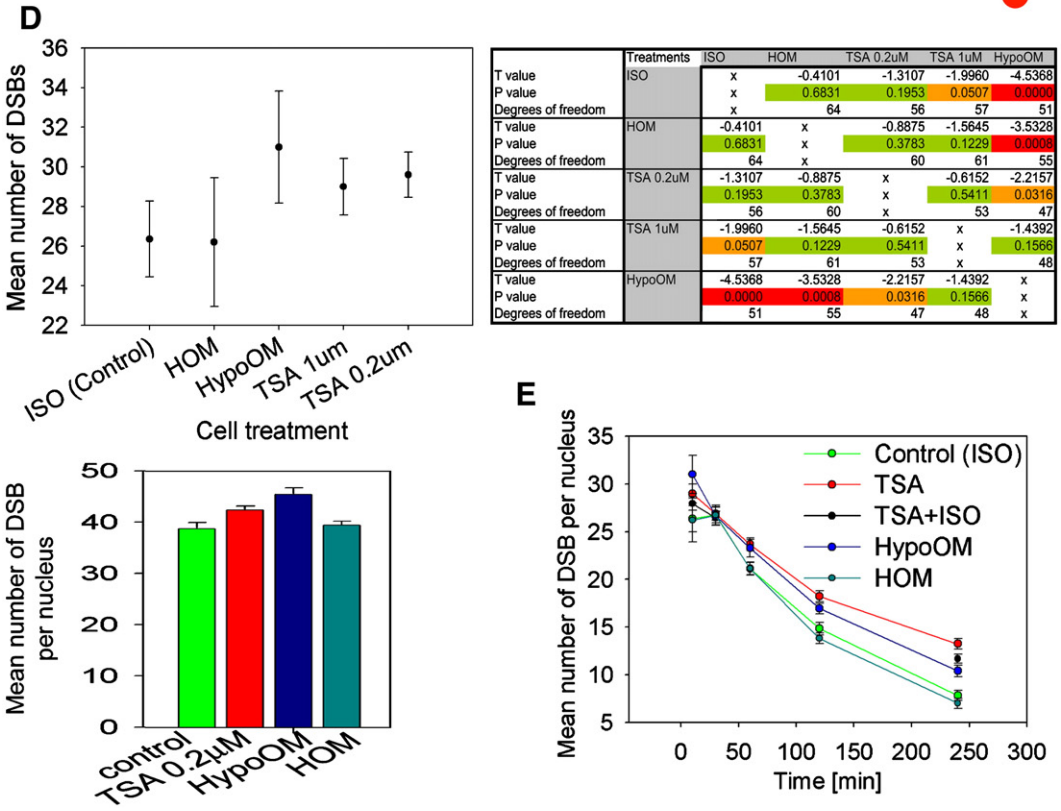

	Treatments	ISO	HOM	TSA 0.2uM	TSA 1uM	HypoOM
T value	ISO	x	-0.4101	-1.3107	-1.9960	-4.5368
P value		x	0.6831	0.1953	0.0507	0.0000
Degrees of freedom		x	64	56	57	51
T value	HOM	-0.4101	x	-0.8875	-1.5645	-3.5328
P value		0.6831	x	0.3783	0.1229	0.0008
Degrees of freedom		64	x	60	61	55
T value	TSA 0.2uM	-1.3107	-0.8875	x	-0.6152	-2.2157
P value		0.1953	0.3783	x	0.5411	0.0316
Degrees of freedom		56	60	x	53	47
T value	TSA 1uM	-1.9960	-1.5645	-0.6152	x	-1.4392
P value		0.0507	0.1229	0.5411	x	0.1566
Degrees of freedom		57	61	53	x	48
T value	HypoOM	-4.5368	-3.5328	-2.2157	-1.4392	x
P value		0.0000	0.0008	0.0316	0.1566	x
Degrees of freedom		51	55	47	48	x

homogeneous distribution of chromatin than in control cell nuclei. The changes in DSB induction and repair induced by HOM, HypoOM and TSA treatments are summarized in Table 1.

4. Discussion

It is generally believed that open chromatin containing active genes is more sensitive to radiation damage than compact chromatin, however direct proofs are still absent. For the first time, using immunoFISH method, we have directly visualized double-strand breaks (marked by γH2AX) together with functionally and structurally distinct genetic loci and also whole chromosome territories in situ under physiological conditions. Our results on chromatin sensitivity obtained by comparison of functionally and structurally different chromatin domains show (Fig. 5) that condensed chromatin in the anti-RIDGE region (low density of expressed genes) [10] is much less susceptible to DSB induction by γ-rays than decondensed chromatin in the RIDGE, characterized by an extremely high density of highly expressed genes. Chromatin condensation in the anti-RIDGE is 40% higher [4, our unpublished results] than that of the RIDGE (of the same length), and the number of DSBs induced in the anti-RIDGE region was 76% lower than in the RIDGE, despite both regions being the same length. A difference in sensitivity to radiation damage was also observed for chromosomes containing high (HSA19 and HSA11) and low densities of genes (HSA4, HSA18 and HSA2). This difference was, however, not so great (about 50%), probably because neither group of chromosomes contains only condensed or decondensed chromatin, unlike the RIDGE and anti-RIDGE. These results show that chromatin structure is one of the most important factors that determine DNA susceptibility to γ-radiation damage, with decondensed, open, genetically active chromatin being more sensitive. The same conclusions also follow from studies of DSB distribution inside the cell nucleus, as well as in individual chromosomal territories (CTs) (Fig. 4A, C). Simultaneous visualization of γH2AX foci and individual chromosome territories of HSA2, HSA4, HSA11, HSA18 and HSA19 by immunoFISH (Fig. 2C) also revealed that DSB lesions arise preferentially in weakly stained subdomains of the CTs, independently of the average characteristics of the whole chromosome, such as gene density.

We were interested whether, apart from higher amount of proteins in heterochromatin, the only higher chromatin condensation *per se* also contributes to a lower sensitivity of heterochromatin for DSB induction and efficiency of their repair. Therefore, we followed radiation sensitivity of hypercondensed chromatin induced by hyperosmotic conditions without participation of additional proteins. Hyperosmotic treatment is known to condense chromatin [23,24] and, in addition, it inhibits growth of tumor [25] and sensitize cells to radiation [24]. It is therefore important to determine, whether these effects are functionally related, in other words, whether therapeutically induced cell killing is caused by changes of chromatin structure, sensitivity to DSB induction and efficiency of their repair.

Our results show, that short-time exposure of cells to hyperosmotic (HOM) medium induced chromatin hypercondensation (HCC) into a network of bundles separated by a contiguous network of large interchromatin channels (ICC) (Fig. 7C) that was rapidly restored to normal chromatin structure after cell transfer to normal medium as already described by [23]. We expected that HCC would protect DNA against damage from γ-radiation. Contrary to our expectation, the sensitivity of HCC, determined as the total number of γH2AX foci per nucleus, remained the same as that of chromatin in cells irradiated in normal medium (ISO).

Together, these results show that condensed chromatin (functionally usually equivalent to heterochromatin) in the cell nucleus protects DNA against damage by γ-radiation, contrary to hypercondensation induced by HOM. The explanation for these different protective effects of these two types of condensed chromatin could reside in their dissimilar way of compaction, and consequently their distinct structure. Physiological heterochromatin is formed with the assistance of chromatin binding proteins (e.g. HP1) [33,34] and is characterized by specific epigenetic modifications (DNA and histone tail methylation, and absence of histone acetylation, reviewed in [35]); the higher density of linker histone H1 in heterochromatin could also contribute to the observed differences [36,37]. Chromatin binding proteins form the principal protective barrier against ionizing radiation (diminishing the accessibility of radicals to the DNA, and themselves reacting with these radicals) [38,39]. The concentration of DNA-binding proteins is lower in open decondensed chromatin, as it is also the density of chromatin per volume unit [40]. Since these proteins require specific histone modifications to bind to DNA, it is very improbable that their amount per unit of chromatin is increased by chromatin hypercondensation in HOM, and therefore the sensitivity of this HCC remains unchanged. Immunochemical detections of the principal epigenetic markers of constitutive heterochromatin (trimethylated histone H3K9, HP1α and β proteins) as well as those (dimethylated H3K9 and HP1 proteins) determining silenced euchromatin (facultative heterochromatin) show that there are hypercondensed chromatin domains in the HOM-treated nuclei that are intensively labeled by TOPRO-3 (chromatin dye) but not with antibodies against mentioned heterochromatic markers (Fig. 9B). The mechanism of hypercondensation is not yet understood, but a high concentration of cations and the resulting decrease in the negative charge of the DNA backbone may play an essential role [41,42]. HCC is probably formed by the contraction of relaxed chromatin, due to the decrease in the negative charge of the DNA in the high concentration of salts, without the participation of additional proteins. This chromatin is not, therefore, protected against damage, and its sensitivity to ionizing radiation remains the same as that in cells with a normal distribution of hetero- and euchromatin.

Fig. 7. Impact on cell viability, DSB repair, chromatin structure, formation of γH2AX foci and their colocalization with 53BP, of short and prolonged incubation of irradiated cells (1.5 Gy) in media with different osmolarities. (A) Green line: increase in the mean number of DSBs per cell in the dependence on incubation time in HOM. After incubation in HOM, the cells were transferred to isotonic medium for 10 min before fixation to allow development of countable γH2AX foci. Red line: the dependence of annexin positivity (beginning stage of apoptosis) on the period of incubation in HOM. (B) Mean fractions of cells containing unrepaired DSBs after 24 h incubation PI in normal (isotonic) medium. Before transfer to isotonic medium, the cells were incubated in HOM for 10 min, (including irradiation with 1.5 Gy). Control cells were not exposed to HOM. (C) Examples of nuclei irradiated with a dose of 1 Gy, and incubated in media with different osmolarities, showing the formation of γH2AX (green) and its colocalization with 53BP (red) at the sites of DSBs. The first nucleus was irradiated in normal isotonic medium, and incubated in this medium for 10 min PI; the second nucleus was irradiated in HOM and incubated in HOM for 10 min after irradiation; γH2AX (green) and 53BP (red) are dispersed as very small dots with non-overlapping distribution. Only about 4.4% of γH2AX colocalize with 53BP. The third nucleus was incubated in HOM for 10 min before irradiation, irradiated in HOM, and transferred to isotonic medium for the next 10 min PI. Foci of γH2AX (green) colocalizing with 53BP (red) are formed, and the chromatin structure resembles that of a normal nucleus. (D) The mean number of DSBs induced by doses of 1.5 Gy (graph) and 3 Gy (histogram) in human fibroblasts incubated in media with different osmolarities 10 min before irradiation, transferred to isotonic immediately after irradiation for further 10 min and fixed. Evaluation was effected in about 60 nuclei. ISO: isotonic medium; HOM: hyperosmotic medium (570 mOsm); HypoOM: hypoosmotic medium (140 mOsm); TSA: incubation for 12 h before irradiation and for 10 min PI. Histogram: control isotonic (green), TSA 0.2 μM (red), HypoOM (dark blue), HOM (blue). Table: Statistical parameters (unpaired t-test) comparing differences in DSB repair between control cells and cells exposed to media with different osmolarities or to TSA (green: $P > 0.05$, orange: $P \leq 0.05$, red: $P \leq 10^{-3}$). (E) The decrease in the number of DSBs (γH2AX) during 4 h PI. The cells were irradiated with a dose of 1.5 Gy in media of different osmolarities, and at 10 min PI transferred to the isotonic medium for different periods of time. Control: normal isotonic medium (290 mOsm); Hyper: hyperosmotic medium (570 mOsm); Hypo: hypoosmotic medium (140 mOsm); TSA: trichostatin A (1 μM) for 12 h before irradiation and after irradiation until cell fixation; TSA-ISO: trichostatin A (0.2 μM) for 12 h before irradiation and transfer to isotonic medium 10 min PI.

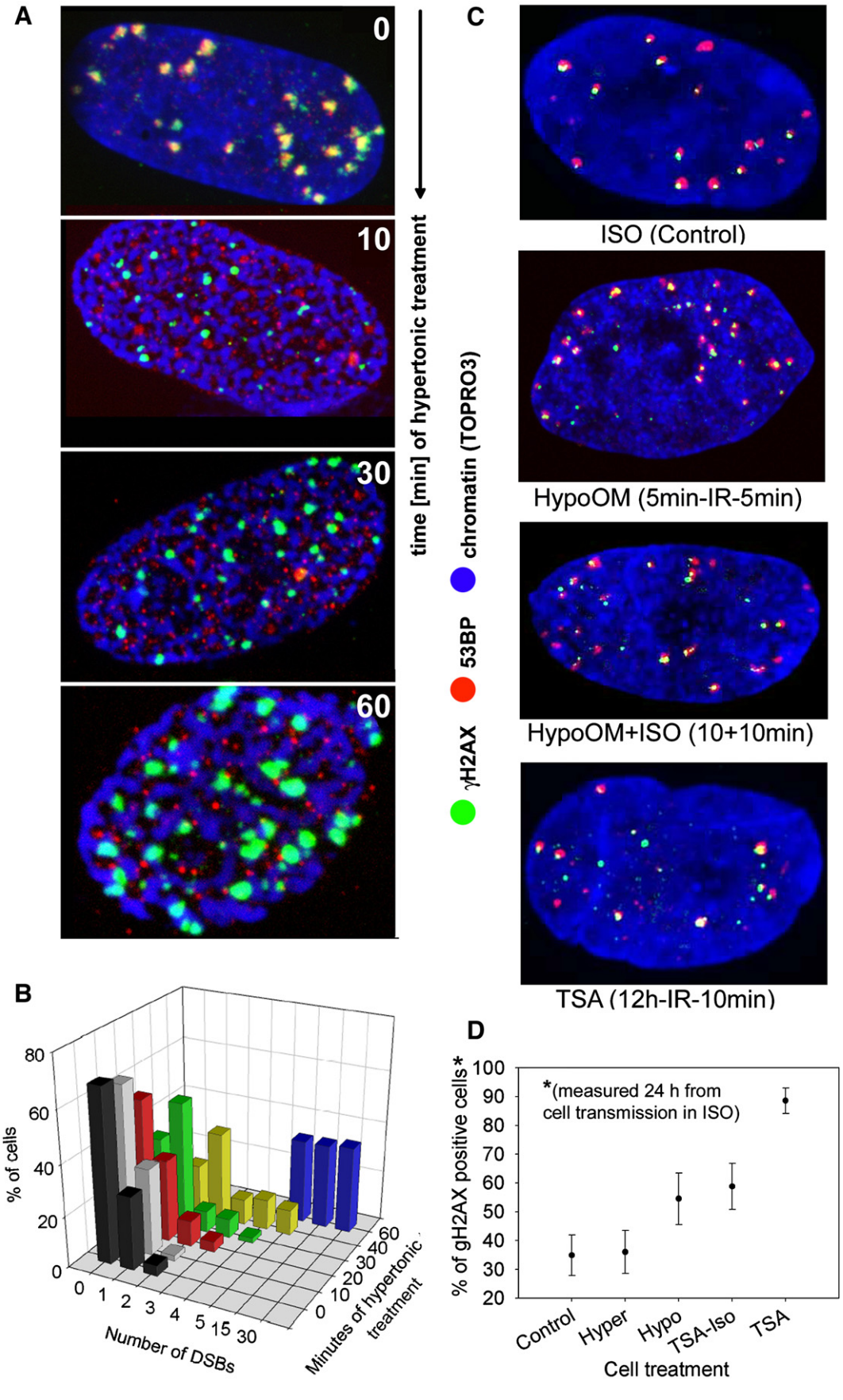
A
0
10
30
60
time [min] of hypertonic treatment
chromatin (TOPRO3)
53BP
γH2AX
C
ISO (Control)
HypoOM (5min-IR-5min)
HypoOM+ISO (10+10min)
TSA (12h-IR-10min)
B
% of cells
Number of DSBs
Minutes of hypertonic treatment
D
% of gH2AX positive cells*
*(measured 24 h from cell transmission in ISO)
Control
Hyper
Hypo
TSA-Iso
TSA
Cell treatment

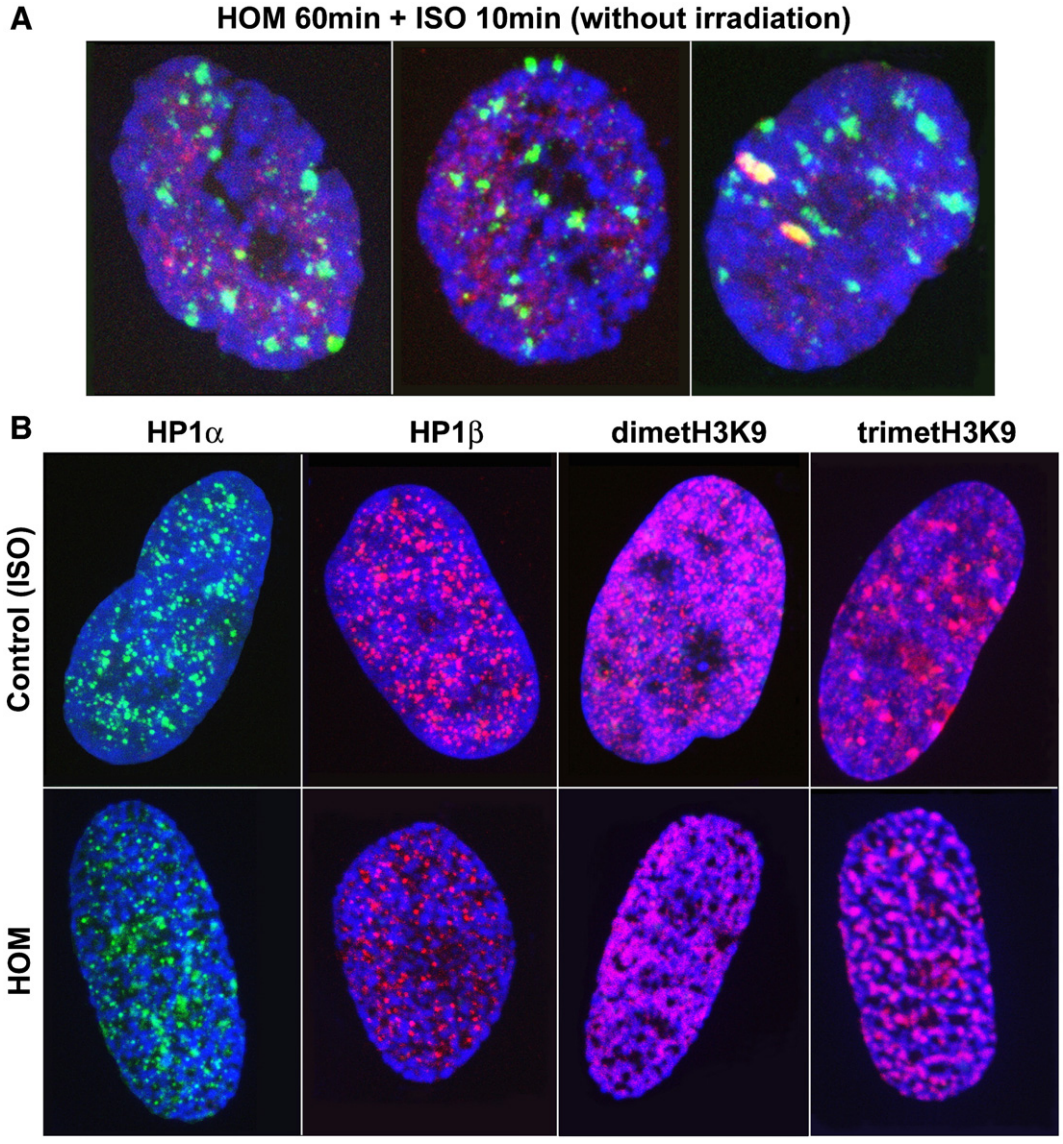

Fig. 9. Induction of γH2AX foci in nuclei of non-irradiated human fibroblasts exposed to HOM for 60 min and nuclear distribution of epigenetic markers of constitutive and facultative heterochromatin compared for HOM-treated (10 min) and control cells. (A) Examples of three nuclei exposed to HOM for 60 min followed by 10 min incubation in normal medium before cell fixation. Green foci of γH2AX indicate induced DSBs, small red dots represent 53BP. The colocalization of two of these foci is seen in the third nucleus, indicating that the nucleus is still surviving, contrary to the first two nuclei. However, neither the third nucleus is completely recovered from the long HOM-treatment as reflected in the incompletely restored chromatin texture. The chromatin of the first two nuclei still remains completely hypercondensed, indication initiation of apoptosis. (B) Immunochemical detection of epigenetic markers of condensed chromatin in control and hypercondensed nuclei (incubated for 10 min in HOM before fixation). Chromatin is labeled by TOPRO-3 (blue), HP1 α (green), HP1β, dimethylated histone H3K9 and trimethylated H3K9 are red. It can be seen that there are hypercondensed chromatin domains also in the HOM-treated nuclei that are intensively labeled by TOPRO-3 (chromatin dye) but not by the antibodies against to the mentioned heterochromatic proteins. This indicates that HOM-induced hypercondensed chromatin is formed without participation of heterochromatic proteins, contrary to physiological heterochromatin.

Exposure of cells to HOM for 10 min, unlike prolonged exposure, did not influence either DSB induction or DSB repair after their transfer to ISO (Fig. 7). However HOM prevented DSB repair and colocalization of repair proteins with γH2AX foci (Fig. 7). The results of Albiez et al. [23] show stalling of other physiological processes such as transcription and replication in HOM, probably as a result of an inhibitory effect of the increased ionic concentration. A high concentration of ions can probably inhibit the activity of many enzymes; it could also alter mutual interactions among proteins, between proteins and DNA, and reduce protein movements [43],

Fig. 8. DSB induction and repair in γ-irradiated (1.5 Gy) human skin fibroblasts relative to the time of these cells exposure to the media with different osmolarities and in the presence of TSA. (A) Examples of irradiated nuclei incubated for different periods of time in HOM, showing the formation of γH2AX (green) foci that do not colocalize with 53BP (red). Emerging colocalization seems to be accidental because of a large amount of red foci and the increasing size of green foci. 4.4%, 14% and 12.6% of green foci colocalize with red foci after 10, 30 and 60 min of cells exposure to HOM, respectively. The first nucleus (control) was incubated for 10 min PI in isotonic medium (0 min in HOM). (B) Distribution of cells with various numbers of DSBs induced by exposure to HOM for different times (0–60 min) and than transferred to isotonic medium for 24 h before evaluation. (C) Changes of chromatin structure, formation of γH2AX foci and their colocalization with DSB-repair proteins in media with different osmolarities: ISO (control): incubation in isotonic medium for 10 min; HypoOM (5 min – IR – 5 min): incubation for 5 min in hypoosmotic medium before, during and after irradiation; HypoOM + ISO (10 + 10 min): incubation 10 min before and during irradiation in hypoosmotic medium, followed by 10 min incubation PI in isotonic medium; TSA (12 h – IR – 10 min): incubation with 1 μm TSA 12 h before irradiation and 10 min PI, including irradiation. (D) Mean fractions of cells containing unrepaired DSBs after 24 h incubation PI in normal (isotonic) medium. Before transfer to isotonic medium, the cells were incubated for 10 min, including irradiation in media of different osmolarities. Incubation with 1 μm TSA was for 12 h before and 24 h after irradiation (TSA), or for 12 h before and only 10 min after irradiation (TSA-Iso), followed by transfer to isotonic medium for 24 h.

Table 1
Comparison of changes of chromatin structure, DSB induction and efficiency of DSB repair induced by hypertonic (HOM), hypotonic (HypoOM) and trichostatin (TSA) treatments

Treatment of cells before and during irradiation (1.5 Gy)	No. of DSBs		Chromatin structure	γH2AX foci	Colocalization of γH2AX foci with repair proteins	Reversibility of changes induced in chromatin structure after transmission to isotonic	The rate of DSB repair after transmission to isotonic
Isotonic (control)	26.4	100%	Normal	+	+		
HOM	26.2	99.24%	Changed[a]	− (early PI) + (20min PI[b])	−	Rapid	Rapid (as in control)
HypoOM	31.0	117.42%	Changed[c]	+	+	Very slow	Very slow
TSA (0.2 μM)	29.0	109.85%	Slightly changed[d]	+	+	Slow	Very slow
TSA (1.0 μM)	29.6	112.12%	Slightly changed[d]	+	+	Slow	Very slow

[a] Condensed bundles encompassed by wide channels of interchromatin space, unstained by chromatin dyes.
[b] Foci started to appear approximately 20 min PI and their size continually increased to values slightly larger than in control cells.
[c] Swelled bundles of condensed chromatin encompassed by thinner channels filled with decondensed chromatin.
[d] Chromatin more diffused and locally more decondensed.

which could result in interruption of physiological functions, including DSB repair. In accordance with this supposition is our observation that well developed foci of γH2AX colocalizing with 53BP in irradiated cells incubated for 20 min in ISO medium disappear, and are replaced by many small dots of both proteins, which do not colocalize with each other after transferring cells into HOM for 10 min (not shown).

We observed that longer (>10 min) exposure of irradiated and also of unirradiated cells to HOM results in an increase in the number of DSBs and annexin positivity (Figs. 7A and 8A, B). This indicates that HOM poses a stress for the cells that could be intensified by the presence of unrepaired DSBs. If these conditions persist for a longer time than can be tolerated by the cell, it is forced into apoptosis. Additional DSBs detected in cells exposed to HOM could probably be induced by nucleases, activated in the early stages of apoptosis [44,45], but also by the loss of water and changes in chromatin conformation. The above described effects of hypertonic, especially inhibition of DSB repair and secondary damage of chromatin, thus could explain recently described successful therapy of VX2 liver carcinoma in rabbits, by injection of hypertonic solution [25]. Summarizing these results, we propose that the increased radiosensitivity of cells exposed to HOM [24] is brought about by inhibition of DSB repair, leading to apoptosis and not by the increased induction of DSBs by radiation. It is necessary to note that results obtained for hypertonic treatment exceeding about 15 min brings new important information concerning the synergic killing of irradiated cells but are not convenient for the study of physiological processes (e.g. DSB repair).

Irradiation of cells in hypoOM followed by short (10 min) exposure to this medium led to a significant increase in DSB induction, as well as reduced rate of repair after the transfer of cells to ISO ($P = 10e^{-3}$) (Fig. 7D, E). The chromatin structure of cells incubated in hypoOM was noticeably changed, forming swollen bundles of condensed chromatin, branched throughout the nucleus in the similar way as bundles of hypercondensed chromatin in cells exposed to HOM (Fig. 8C). The similarity of branched condensed chromatin structure in hypoOM to the hypercondensed bundles induced in HOM supports the concept of a global 3D chromatin network, established in early G_1, as proposed by Gerlich et al. [46] and Walter et al. [47], and also supported by the findings of Albiez et al. [23], who showed the stability of chromatin bundles during repeated NCC-HCC-NCC cycles (NCC, normally condensed chromatin). Contrary to HCC induced during the short-time (<10 min) incubation in HOM, which is completely reversible after transfer of the cells to ISO, chromatin changes developed in hypoOM return to normal (Fig. 8C) only very slowly (2 h PI or more). The explanation for this slow reversibility could reside in the more profound changes of chromatin structure: The decrease of cation concentration probably results in destabilization of nucleosome structure, especially in decondensed chromatin. It has been shown that nucleosome conformation is strongly dependent on ionic strength [48]. A low concentration of ions thus could influence the structure of DNA, via modified interactions of its phosphate groups with basic amino-acid residues of the histone octamer [49]. Such a disturbance of physiological chromatin structure that persists even when the hypoOM conditions were removed could be responsible for the low efficiency of DSB repair.

As HDAC inhibitors are currently used in clinical trials, because of their promising anticancer effects [50], and are used as additives, or synergistic with conventional cancer therapies such as radiotherapy [51], we used one of these inhibitors, TSA, to evaluate DSB induction and repair efficiency in human fibroblasts. The effect of TSA was evaluated for whole chromatin, and separately for condensed and decondensed chromatin of selected chromosomes, RIDGE and anti-RIDGE regions (Figs. 5 and 6). Surprisingly, we observed only a small non-significant increase of DSB induction in whole nuclei of cells exposed to TSA for 12 h before irradiation (with doses of 1.5 Gy and 3 Gy of γ-rays) and in chromosomes with more condensed chromatin (HSA4, HSA18 and HSA2), while the number of DSBs was the same as in untreated control cells in chromosomes with a high level of decondensed chromatin. The increased number of DSBs induced in condensed chromatin of cells treated with TSA before irradiation could be related to globally increased acetylation of histones, leading to reversible decondensation of dense chromatin regions, as found by Tóth et al. [28]. Our observation of a more homogenous distribution of chromatin in nuclei exposed to TSA (Fig. 8C) and a slightly higher induction of DSBs in heterochromatic chromosomes (Fig. 6), is consistent with the observed TSA-induced relaxation of condensed chromatin domains containing several megabase pairs of DNA [28].

The significant decrease of DSB-repair efficiency in cells treated with TSA, especially in the decondensed chromatin of the RIDGE, contrasts with the observation of only small changes in DSB induction. In this region, the number of DSBs was reduced 5.2 times after 4 h of repair (relative to the values immediately PI) in untreated cells, but was only reduced 2.9 times in cells treated with 1 μM TSA. Similarly, for chromosomes containing a high density of genes, and therefore a higher level of decondensed chromatin (HSA19 and HSA11), this reduction was 4.6 times in untreated cells, and only 2.7 times in TSA-treated cells. For chromosomes with a low gene density and more condensed chromatin, the difference in repair efficiency between the untreated and treated cells was lower 3 times for HSA2 and 2.3 times for HSA18 and HSA4. The small difference between the TSA-treated and untreated cells was found also for the anti-RIDGE (2.1 times and 1.7 times, respectively). These results show a significant dependence of the repair efficiency on chromatin structure in untreated cells, and a decrease of this efficiency, especially in open chromatin, in TSA-treated cells.

Numerous studies have already shown that HDAC inhibitors can enhance radiosensitivity of various cancer cell lines [51,52], but the mechanism by which HDAC inhibitors enhance this sensitivity in human cells remains unclear. The long-lasting acetylation of histones, creating open chromatin, could be the main reason for the slowdown of DSB repair in cells exposed to TSA. Our earlier results [6] showed

that increased acetylation in the region of γH2AX foci (developed immediately after DSB induction) was soon replaced by histone modification typical for condensed chromatin (decreased acetylation of H4K5 and increased methylation of H3K9). These relatively rapid changes in epigenetic modification of both histones in the proximity of DSBs indicate the necessity for conversion from less to more condensed chromatin during repair. This condensation is probably not possible in the presence of HDAC inhibitor, and could lead to decreases in repair efficiency. In addition, repair efficiency could also be influenced by more indirect effects of increased histone acetylation, including recruitment of chromatin-remodeling complexes [53,54] and other chromosomal proteins [55] that modify higher-order chromatin conformation.

Acknowledgements

We thank Sandra Goetze for kindly providing us the probes for RIDGE and anti-RIDGE regions. This work was supported by the Grant Agency of the Czech Republic (204/06/P349), the GAAV of the Czech Republic (IAA500040802, 1QS500040508), the Academy of Sciences of the Czech Republic (AV0Z50040507, AV0Z50040702), and the Ministry of Education of the Czech Republic (LC535).

References

[1] S. Boyle, S. Gilchrist, J.M. Bridger, U.L. Mahy, J.A. Ellis, W.A. Bickmore, The spatial organization of human chromosomes within the nuclei of normal and emerin-mutant cells, Hum. Mol. Genet. 10 (2001) 211–219.
[2] M. Cremer, J. von Haase, T. Volm, A. Brero, G. Kreth, J. Walter, C. Fisher, I. Solovei, C. Cremer, T. Cremer, Non-random radial higher-order chromatin arrangements in nuclei of diploid human cells, Chromosome Res. 9 (2001) 541–567.
[3] S. Kozubek, E. Lukášová, P. Jirsová, I. Koutná, M. Kozubek, A. Gaňová, E. Bártová, M. Falk, R. Paseková, 3D structure of human genome: order in randomness, Chromosoma 111 (2002) 321–331.
[4] S. Goetze, J. Mateos-Langerak, H. Gierman, W. de Leeuw, O. Giromus, M.H.G. Indemans, J. Koster, V. Ondřej, R. Versteeg, R. van Driel, The three-dimensional structure of human interphase chromosomes is related to the transcriptome map, Mol. Cell. Biol. 27 (2007) 4475–4487.
[5] Y. Ziv, D. Bielopolski, Y. Galanty, C. Lukas, Y. Taya, D.C. Schultz, J. Lukas, S. Bekker-Jensen, J. Bartek, Y. Shiloh, Chromatin relaxation in response to DNA double-strand breaks is modulated by a novel ATM- and KAP-1 dependent pathway, Nature Cell Biol. 8 (2006) 870–876.
[6] M. Falk, E. Lukasova, B. Gabrielova, V. Ondřej, S. Kozubek, Chromatin dynamics during DSB repair, Biochim. Biophys. Acta 1773 (2007) 1534–1545.
[7] O. Fernandez-Capetillo, A. Lee, M. Nussenzweig, A. Nussenzweig, H2AX: the histone guardian of the genome, DNA Repair 3 (2004) 959–967.
[8] R. Kanaar, J.H. Hoeijmakers, D.C. van Gent, Molecular mechanisms of DNA double strand breaks repair, Trends Cell Biol. 8 (1998) 483–489.
[9] B. Eliot, M. Jasin, Double-strand breaks and translocations in cancer, Cell. Mol. Life Sci. 59 (2002) 373–385.
[10] H. Caron, B. van Schaik, M. van der Mee, F. Baas, G. Riggins, P. van Sluis, M.C. Hermus, R. van Asperen, K. Boon, P.A. Voute, R. Versteeg, et al., The human transcriptome map: clustering of highly expressed genes in chromosomal domains, Science 291 (2001) 1289–1292.
[11] R. Versteeg, B.D.C. van Schaik, M.F. van Batenburg, M. Roos, R. Monajemi, H. Caron, H.J. Bussemaker, A.H.C. van Kampen, The human transcriptome map reveals extremes in gene density, intron length, GC content and repeat pattern for domains of highly and weakly expressed genes, Genome Res. 13 (2003) 1998–2004.
[12] J. Surrallés, S. Sebastian, A.T. Natarajan, Chromosomes with high gene density are preferentially repaired in human cells, Mutagenesis 12 (1997) 437–442.
[13] F. Daroudi, J. Fomina, M. Meijers, A.T. Natarajan, Kinetics of the formation of chromosome aberrations in X-irradiated human lymphocytes using PCC and FISH, Mutat. Res. 404 (1998) 55–65.
[14] G. Iliakis, G.E. Pantelias, R. Seaner, Effect of arabinofuranosyladenine on radiation induced chromosome damage in plateau-phase CHO cells measured by premature chromosome condensation: implication for repair and fixation of alpha-PLD, Radiat. Res. 114 (1988) 361–378.
[15] L. Metzger, G. Iliakis, Kinetics of DNA double-strand break repair through the cell cycle as assayed by pulsed field gel electrophoresis in CHO cells, Int. J. Rad. Biol. 59 (1991) 1325–1339.
[16] D. Sproul, N. Gilbert, W.A. Bickmore, The role of chromatin structure in regulating the expression of clustered genes, Nat. Rev. Genet. 6 (2005) 775–781.
[17] H. Tanabe, F.A. Habermann, I. Solovei, M. Cremer, T. Cremer, Non-random radial arrangement of interphase chromosome territories: evolutionary considerations and functional implications, Mutat. Res. 504 (2002) 37–45.
[18] E. Gazave, P. Gautier, S. Gilchrist, W.A. Bickmore, Does radial nuclear organisation influence DNA damage? Chromosome Res. 13 (2005) 377–388.
[19] E.P. Rogakou, D.R. Pilch, A.H. Orr, V.S. Ivanova, W.M. Bonner, DNA double strand breaks induce histone H2AX phosphorylation on serine 139, J. Biol. Chem. 273 (1998) 5858–5868.
[20] C.J. Bakkenist, M.B. Kastan, DNA damage activates ATM through intermolecular autophosphorylation and dimmer association, Nature 421 (2003) 499–506.
[21] A. Pombo, P. Cuello, W. Schul, J.B. Yoon, R.G. Roeder, P.R. Cook, S. Murphy, Regional and temporal specialization in the nucleus: a transcriptionally-active nuclear domain rich in PTF, Oct1 and PIKA antigens associated with specific chromosomes early in the cell cycle, EMBO J. 17 (1998) 1768–1778.
[22] T. Reitsema, D. Klokov, J.P. Banáth, P.L. Olive, DNA-PK is responsible for enhanced phosphorylation of histone H2AX under hypertonic conditions, DNA Repair 4 (2005) 1172–1181.
[23] H. Albiez, M. Cremer, C. Tiberi, L. Vecchio, L. Schermelleh, S. Dittrich, K. Kupper, B. Joffe, T. Thormeyer, J. von Hase, S. Yang, K. Rohr, H. Leonhardt, I. Solovei, C. Cremer, S. Facan, T. Cremer, Chromatin domains and the interchromatin compartments from structurally defined and functionally interacting nuclear networks, Chromosome Res. 14 (2006) 707–733.
[24] C.M. Dettor, W.C. Dewey, L.F. Winans, J.S. Noel, Enhancement of X-ray damage in synchronous Chinese hamster cells by hypertonic treatments, Radiat. Res. 52 (1972) 352–372.
[25] Y.C. Lin, J.H. Chen, K.W. Han, W.C. Shen, Ablation of liver tumor by injection of hypertonic saline, AJR Am. J. Roentgenol. 184 (2005) 212–219.
[26] D. Cerna, K. Camphausen, P.J. Tofilon, Histone deacetylation as a target for radiosensitization, Curr. Top Dev. Biol. 73 (2006) 243–251.
[27] K. Camphausen, P.J. Tofilon, Inhibition of histone deacetylation: a strategy for tumor radiosensitization, J. Clin. Oncol. 25 (2007) 4051–4056.
[28] K.F. Tóth, T.A. Knoch, M. Wachsmuth, M. Frank-Stöhr, M. Stöhr, C.P. Bacher, G. Müller, K. Rippe, Trichostatin A-induced histone acetylation causes decondensation of interphase chromatin, J. Cell Sci. 117 (2004) 4277–4287.
[29] M. Kozubek, S. Kozubek, E. Lukasova, A. Mareckova, E. Bartova, M. Skalnikova, A. Jergova, High-resolution cytometry of FISH dots in interphase cell nuclei, Cytometry 36 (1999) 279–293.
[30] M. Kozubek, S. Kozubek, E. Lukasova, E. Bartova, M. Skalnikova, P. Matula, P. Matula, P. Jirsova, A. Cafourkova, I. Koutna, Combined confocal and wide-field high-resolution cytometry of fluorescent in situ hybridization-stained cells, Cytometry 45 (2001) 1–12.
[31] Y. Kuwada, T. Sakamura, A contribution to the colloidchemical and morphological study of chromosomes, Protoplasna 1 (1927) 239–254.
[32] O. Bank, Abhaenigigkeit der Kernstruktur von der Ionenkonzentration, Protoplasma 32 (1939) 20–30.
[33] A.J. Banister, P. Zegerman, J.F. Partridge, E.A. Miska, J.O. Thomas, R.C. Allshire, T. Kouzarides, Selective recognition of methylated lysine 9 on histone H3 by the HP1 chromo domain, Nature 410 (2001) 120–124.
[34] M. Lachner, D. O, Carroll, S. Rea, K. Mechtler, T. Jenuwein, Methylation of histone H3 lysine 9 creates a binding site for HP1 protein, Nature 410 (2001) 116–120.
[35] E.J. Richards, S.C. Elgin, Epigenetics codes for heterochromatin formation and silencing: rounding up the usual suspects, Cell 108 (2002) 489–500.
[36] J. Tazi, A. Bird, Alternative chromatin structure at CpG islands, Cell 60 (1990) 909–920.
[37] J. Zlatanova, P. Caiafa, K. van Holde, Linker histone binding and displacement: versatile mechanism for transcriptional regulation, FASEB J. 14 (2000) 1697–1704.
[38] M. Bĕgusova, N. Gillard, D. Sy, B. Castaing, M. Charlier, M. Spotheim-Maurizo, Radiolysis of DNA–protein complexes, Radiat. Phys. Chem. 72 (2005) 265–270.
[39] M. Davídková, V. Štisová, S. Goffinont, N. Gillard, B. Castaing, M. Spotheim-Maurizot, Modification of DNA radiolysis by DNA-binding proteins: structural aspects, Rad. Protect. Dosim. 10 (2006) 1–6.
[40] S. Dietzel, K. Zolghadr, C. Hepperger, A.S. Belmont, Differential large-scale chromatin compaction and intranuclear positioning of transcribed versus non-transcribed transgene arrays containing beta-globin regulatory sequences, J. Cell Sci. 117 (2004) 4603–4614.
[41] J.C. Hansen, Conformational dynamics of the chromatin fibre in solution: determinants, mechanisms and functions, Annu. Rev. Biophys. Biomol. Struct. 31 (2002) 361–392.
[42] P.J. Horn, C.L. Peterson, Molecular biology. Chromatin higher order folding-wrapping up transcription, Science 297 (2002) 1824–1827.
[43] M. Lund, B. Jönsson, A mesoscopic model for protein–protein interactions in solutions, Biophys. J. 85 (2003) 2940–2947.
[44] J.Z. Parrish, D. Xue, Cuts can kill: the roles of apoptic nucleases in cell death and animal development, Chromosoma 115 (2006) 89–97.
[45] K. Samejima, W.C. Ernshaw, Trashing the genome: the role of nucleases during apoptosis, Nat. Rev. Mol. Cell. Biol. 6 (2005) 677–688.
[46] D. Gerlich, J. Beaudouin, B. Kalbfess, N. Daigle, R. Eils, J. Ellenberg, Global chromosome positions are transmitted through mitosis in mammalian cells, Cell 112 (2003) 751–764.
[47] J. Walter, L. Schermelleh, M. Cremer, S. Tashiro, T. Cremer, Chromosome order in HeLa cells during mitosis and early G1, but is stably maintained during subsequent interphase stages, J. Cell Biol. 160 (2003) 685–697.
[48] T.J. Richmond, C.A. Davey, The structure of DNA in the nucleosome core, Nature 423 (2003) 145–150.
[49] G.S. Manning, Is a small number of charge neutralizations sufficient to bend nucleosome core DNA onto its superhelical ramp? J. Am. Chem. Soc. 125 (2003) 15087–15092.
[50] R.L. Piekarz, R.W. Robey, Z. Zhan, G. Kayastha, A. Sayah, A.H. Abdeldaim, T-cell lymphoma as a model for the use of histone deacetylase inhibitors in cancer therapy: impact of depsipeptide on molecular markers, therapeutic targets, and mechanisms of resistance, Blood 103 (2004) 4636–4643.

[51] K. Camphausen, W. Burgan, M. Cerra, K.A. Oswald, J.B. Trepel, M.J. Lee, Enhanced radiation-induced cell killing and prolongation of gammaH2AX foci expression by the histone deacetylase inhibitor MS-275, Cancer Res. 64 (2004) 316–321.
[52] T.C. Karagiannis, H. Kn, A. El-Osta, Disparity of histone deacetylase inhibition on repair of radiation-induced DNA damage on euchromatin and constitutive heterochromatin, Oncogene 25 (2007) 3963–3971.
[53] P.T. Georgel, T. Tsukiyama, C. Wu, Role histone tails in nucleosome remodelling by Drosophila NURF, EMBO J. 16 (1997) 4717–4726.
[54] C. Logie, C. Tse, J.C. Hansen, C.L. Peterson, The core histone N-terminal domains are required for multiple rounds of catalytic chromatin remodelling by SWI/SNF and RSC complexes, Biochemistry 38 (1999) 2514–2522.
[55] C. Maison, D. Bailly, A.H. Peters, J.P. Quivy, D. Roche, A. Taddei, M. Lachner, T. Jenuvein, G. Almouzni, Higher-order structure in pericentric heterochromatin involves a distinct pattern of histone modification and RNA component, Nat. Genet. 30 (2002) 329–334.
[56] M. Costantini, O. Clay, F. Auletta, G. Bernardi, An isochore map of human chromosomes, Genome Res. 16 (2006) 536–541.